

## Three-dimensional relativistic structure for quarkonium states

X. Q. Zhu\* and F. C. Khanna

*Theoretical Physics Institute, Department of Physics, University of Alberta, Edmonton, Alberta, Canada, T6G 2J1  
and TRIUMF, 4004 Wesbrook Mall, Vancouver, British Columbia, Canada, V6T 2A3*

R. Gourishankar and R. Teshima

*Department of Physics, University of Alberta, Edmonton, Alberta, Canada, T6G 2J1*

(Received 3 August 1992)

A three-dimensional relativistic equation is used to calculate the quarkonium spectra. The kernel is the one obtained by projecting the Bethe-Salpeter (BS) kernel with both fermions being on the mass shell. The potential in the momentum representation is assumed to have a Coulomb part with high-momentum cutoff and a confinement part regularized by a small mass parameter. A complete Dirac bilinear covariant set is used to describe the spin structure of the potential. The quarkonium wave function is expanded in terms of the free Dirac spinors which are classified by the irreducible representation of the Lorentz group. Most of the quarkonium states are embedded in the continuum which exists due to the finite barrier of the confinement potential. Several sets of parameters for qualitatively fitting the experimental data are considered. The results show that the axial-vector and tensor bilinear covariants have to be included in the spin structure of the original BS kernel to explain the spectra of the quarkonium system. This property is different from that in the Schrödinger formalism, where the spin-dependent forces originate from relativistic corrections of vector covariants. The mixing of  $S$  and  $D$  components in the wave function of the  $J/\psi$  system is shown to be sensitive to the presence of the axial-vector and tensor components of the potential.

PACS number(s): 14.40.Jz, 11.10.Qr, 11.10.St, 12.40.Qq

### I. INTRODUCTION

The Schrödinger formalism with various modified forms of the phenomenological potential has provided an overwhelmingly successful approach for the description of quarkonium and meson states. (See Refs. [1–3] and references quoted therein.) However, even from a purely phenomenological point of view, one always feels a great deal of uneasiness about using the Schrödinger formalism. First, the dynamical input in the three-dimensional nonrelativistic potential does not distinctly link up with those in the covariant kernel in nonperturbative procedures. Although the nonperturbative procedure [for example, the Bethe-Salpeter (BS) equation] [4,5] by itself is completely phenomenological, it is highly desirable that the dynamical parameters in these two procedures have a clear connection. Second, it is inevitable to use the BS amplitude with a covariant spin structure in the calculation of the external current matrix elements between hadron states [6,7]. There is quite a vague relationship between the BS amplitudes and nonrelativistic wave functions. As a result, a plentiful knowledge of the Schrödinger wave functions is not sufficient in the phenomenological analysis of the standard model.

There are infinite ways to project the BS equation into a three-dimensional relativistic equation [8–11]. Each of

them has the same mathematical structure as the Schrödinger equation and no more difficulty in numerical computation than solving the Schrödinger equation. However, the spin structures in these three-dimensional relativistic equations are Lorentz covariant and the potentials in these equations are directly related to the BS kernel. Therefore it makes a great deal of sense to establish quarkonium and meson structure in the three-dimensional relativistic equation. It will definitely help us to understand the relationship between two types of phenomenological approaches and make the bound-state wave functions a much more active ingredient in the calculations of the external current matrix elements between hadron states.

Among all of these three-dimensional relativistic equations, the equation with an on-shell BS kernel is the most simple and, probably, special [8]. The main feature of this equation is that both quarks of the hadron in the kernel are on the mass shell. So we are able to expand the hadron wave function in terms of free Dirac spinors. All the quantum numbers such as orbital angular momentum and the internal spin in the nonrelativistic theory can be preserved in the Lorentz-covariant representation. It becomes very convenient to compare the results in the nonrelativistic theory to the wave function in the covariant representation. In other types of the three-dimensional relativistic equations such as the one with one fermion being on the mass shell [9] or the one-time relativistic equation [10], the constituent quarks are off the mass shell; therefore, the free-Dirac-spinor representation is not complete any more. One has to use Llewellyn-

---

\*Present address: Dept. of Physics, Brooklyn College, City University of New York, Brooklyn, NY 11210.

Smith's representation [12] for solving these equations and classify the hadron states only by space and charge or  $G$  parity. However, once we have a solution in terms of the covariant Dirac spinors, it will be direct to observe its connection to the complete basis of  $4 \times 4$   $\gamma$  matrices [12].

In Sec. II we review the relationship of the BS and three-dimensional relativistic equations to have a clear starting point for the on-mass-shell projection. A potential including a Coulomb part with a large momentum cutoff  $\Lambda_{\text{QCD}}$  and a confinement part with an infrared regularization, small parameter  $\mu$ , is written down. Both potentials are associated with a complete spin structure in terms of bilinear covariants. The wave function is expanded in terms of free Dirac spinors, which are classified by the irreducible representation of the inhomogeneous Lorentz group. Most of the details are collected in Appendix A. The explicit expression of the potential for various quarkonium states is given in Appendix B. Also, the relationship of space and charge parity with the relative angular momentum and spin in the relativistic representation is reviewed. In Sec. III a numerical study of the three-dimensional relativistic equation has been developed. Since the confinement potential with a regularization to take account of the light-cone singularity possesses a barrier with a finite height, most of the excited bound states are embedded in a kind of spurious continuum. These bound states are carefully identified from the continuum by counting nodes of the corresponding wave functions. Several sets of parameters for fitting the experimental spectral data are given. The corresponding wave functions have been obtained and are displayed. From the numerical results and the analysis of the analytical behavior of the kernel in the finite-momentum region, the difference between the Schrödinger formalism and the three-dimensional relativistic approach is explored, which shows that all of the spin-dependent forces in these two approaches have a different origin. Finally, a brief summary is given in Sec. IV.

## II. EQUATION OF MOTION AND THE POTENTIAL

### A. Equation of motion

Let us start with a two-identical-quark system. The three-dimensional relativistic equation of this system can be written as

$$(M - 2E_p)\psi_M(\mathbf{p}) = \int d^3q V(\mathbf{p}, \mathbf{q})\psi_M(\mathbf{q}). \quad (1)$$

$$G'_0(k_1 k_2; k'_1 k'_2) = m^2 \int dM \frac{d^3 p_1 d^3 p_2}{E_{p_1} E_{p_2}} U(k_1 k_2; M \mathbf{p}_1 \mathbf{p}_2) g(M \mathbf{p}_1 \mathbf{p}_2) U(M \mathbf{p}_1 \mathbf{p}_2; k'_1 k'_2) \quad (7)$$

and

$$g(M \mathbf{p}_1 \mathbf{p}_2) = \frac{1}{M - H_1(\mathbf{p}_1) - H_2(\mathbf{p}_2) - i\epsilon}, \quad (8)$$

with  $H_i(\mathbf{p}) = \alpha_i \cdot \mathbf{p} + m\beta_i$ ,  $m$  is the quark mass, and  $E_{p_1}$  and  $E_{p_2}$  in the denominator of (7) are formally introduced to as-

If the BS kernel of the same system is assumed to have a general structure of

$$I(\mathbf{p}, \mathbf{q}) = \sum_j I^j(pq) \Gamma_1^j \otimes \Gamma_2^j, \quad (2)$$

where  $\{\Gamma^j\}$  is the complete basis of the  $4 \times 4$  matrices, then the potential  $V(\mathbf{p}, \mathbf{q})$  in (1) is given by

$$V(\mathbf{p}, \mathbf{q}) = \sum_j I^j(\Delta^2) [\Lambda_1^+(\mathbf{p}) \beta_1 \Gamma_1^j \Lambda_1^+(\mathbf{q})] \otimes [\Lambda_2^+(-\mathbf{p}) \beta_2 \Gamma_2^j \Lambda_2^+(-\mathbf{q})]. \quad (3)$$

Here

$$\Delta^2 = (E_p - E_q)^2 - (\mathbf{p} - \mathbf{q})^2, \quad (4)$$

with  $E_p = (\mathbf{p}^2 + m^2)^{1/2}$  and  $\Lambda^\pm(\mathbf{p})$  represent the projection operators for positive- and negative-energy Dirac spinors given by (A13). There have been many papers during the past four decades to develop a reduction of the BS equation to a three-dimensional relativistic equation including Eqs. (1)–(4). Each of these approaches has its own point of focus. The general context of this topic can be found from the original papers [8] and some review papers [11]. Since Eqs. (1)–(4) play the role of a basic equation of motion for our calculations, it becomes necessary, at the first instant, to review certain important features in the relationship of these equations to the BS equation.

In the BS equation, both fermions are off the mass shell, and so one is working in eight-dimensional space, which includes the two energy variables, the real energy of the two-particle system, and the relative energy variable, which lacks any physical meaning. Let us first introduce a projection operator to restrict the relative energy variable to a certain special value such that

$$U(M \mathbf{k}_1 \mathbf{k}_2; q_1 q_2) = \delta(M - Q) \delta^3(\mathbf{K} - \mathbf{Q}) U_{MK}(\mathbf{k}; q^0 \mathbf{q}), \quad (5)$$

and

$$U_{MK}(\mathbf{k}; q^0 \mathbf{q}) = \delta \left[ \frac{M}{2} - E_{\mathbf{k}} + q^0 \right] \delta^3(\mathbf{k} - \mathbf{q}) \Lambda_1^+(\mathbf{k}_1) \Lambda_2^+(\mathbf{k}_2), \quad (6)$$

where  $Q = q_1 + q_2$ ,  $q = \frac{1}{2}(q_1 - q_2)$ , and the same definition for  $\mathbf{K}$  and  $\mathbf{k}$ . Obviously, this operator projects the spin structure of the two-quark system into two free Dirac spinors and fixes the relative energy variable at  $E_{\mathbf{k}} - M/2$ . Next, we define a Green's function in eight-dimensional space:

sure covariance of the three-dimensional integration. It can be easily checked that the dimensional scale of  $G'_0$  is the same as the product of the two single-particle Feynman Green's functions. Now we turn to the BS equation for the quark-quark scattering amplitude

$$T(k_1 k_2; k'_1 k'_2) = I(k_1 k_2; k'_1 k'_2) + \int I(k_1 k_2; \xi_1 \xi_2) G_0(\xi_1 \xi_2; \eta_1 \eta_2) T(\eta_1 \eta_2; k'_1 k'_2), \quad (9)$$

where the repeated Greek letters indicate the integration variables and omit the corresponding integration symbols. Here the kernel  $I$  is obtained as a summation of all the irreducible Feynman graphs for two-particle initial and final states and  $G_0$  is given by

$$G_0(k_1 k_2; k'_1 k'_2) = S_F(k_1 - k'_1) S_F(k_2 - k'_2). \quad (10)$$

The scattering amplitude will include all the singular terms arising from the two-quark bound states. Since the  $T$  function is independent of any boundary condition, we are able to rearrange Eq. (9) according to the Green's function (7) into the form

$$T(k_1 k_2; k'_1 k'_2) = I'(k_1 k_2; k'_1 k'_2) + \int I'(k_1 k_2; \xi_1 \xi_2) G'_0(\xi_1 \xi_2; \eta_1 \eta_2) T(\eta_1 \eta_2; k'_1 k'_2). \quad (11)$$

The new kernel  $I'$  relates to the original BS kernel  $I$  by

$$I'(k_1 k_2; k'_1 k'_2) = I(k_1 k_2; k'_1 k'_2) + \int I(k_1 k_2; \xi_1 \xi_2) [G_0(\xi_1 \xi_2; \eta_1 \eta_2) - G'_0(\xi_1 \xi_2; \eta_1 \eta_2)] I'(\eta_1 \eta_2; k'_1 k'_2). \quad (12)$$

Multiplying by the projection operator (5) from the left and the right on both sides of Eq. (11) and integrating over with all the variables, we obtain an equation of the form

$$\hat{T}(M \mathbf{k}_1 \mathbf{k}_2; M' \mathbf{k}'_1 \mathbf{k}'_2) = \hat{T}'(M \mathbf{k}_1 \mathbf{k}_2; M' \mathbf{k}'_1 \mathbf{k}'_2) + m^2 \int d\varepsilon \frac{d^3 \xi_1 d^3 \xi_2}{E_{\xi_1} E_{\xi_2}} \hat{T}'(M \mathbf{k}_1 \mathbf{k}_2; \varepsilon \xi_1 \xi_2) g(\varepsilon \xi_1 \xi_2) \hat{T}(\varepsilon \xi_1 \xi_2; M' \mathbf{k}'_1 \mathbf{k}'_2). \quad (13)$$

Here we have used expression (7) for  $G'_0$  and introduced the notation

$$\hat{O}(M \mathbf{k}_1 \mathbf{k}_2; M' \mathbf{k}'_1 \mathbf{k}'_2) = \int U(M \mathbf{k}_1 \mathbf{k}_2; \xi_1 \xi_2) O(\xi_1 \xi_2; \eta_1 \eta_2) U(\eta_1 \eta_2; M' \mathbf{k}'_1 \mathbf{k}'_2), \quad (14)$$

which represents a projection of the eight-dimensional Feynman amplitude to the surface of eight-dimensional space, i.e., a seven-dimensional amplitude without the relative energy variable. Considering that the total four-momentum is conserved both in the projection operator (5) and the usual Feynman amplitude, we can factorize this  $\delta$  function out of Eqs. (11)–(14). In other words,

$$O(k_1 k_2; k'_1 k'_2) = \delta^4(K - K') O_K(k; k'), \quad (15)$$

$$\hat{O}(M \mathbf{k}_1 \mathbf{k}_2; M' \mathbf{k}'_1 \mathbf{k}'_2) = \delta(M - M') \delta^3(K - K') \hat{O}_{MK}(\mathbf{k}; \mathbf{k}'), \quad (16)$$

where

$$\hat{O}_{MK}(\mathbf{k}; \mathbf{k}') = \Lambda_1^+ \left[ \frac{\mathbf{K}}{2} + \mathbf{k} \right] \Lambda_2^+ \left[ \frac{\mathbf{K}}{2} - \mathbf{k} \right] O_{MK} \left[ E_k - \frac{M}{2} \mathbf{k}; E_{k'} - \frac{M}{2} \mathbf{k}' \right] \Lambda_1^+ \left[ \frac{\mathbf{K}}{2} + \mathbf{k}' \right] \Lambda_2^+ \left[ \frac{\mathbf{K}}{2} - \mathbf{k}' \right]. \quad (17)$$

In getting this expression, we have used the explicit form of the projection operator (6). Substituting (16) into (13) and taking the center-of-mass frame  $\mathbf{K} = 0$ , we have

$$\hat{T}_M(\mathbf{k}; \mathbf{k}') = \hat{T}'_M(\mathbf{k}; \mathbf{k}') + \int d^3 \xi \hat{T}'_M(\mathbf{k}; \xi) g_M(\xi) \hat{T}_M(\xi; \mathbf{k}'), \quad (18)$$

where we have dropped the factor  $m^2/E_\xi^2$  by remembering that the normalization of the Dirac spinors should be  $u^\dagger u = 1$  instead of  $\bar{u}u = 1$ , as is usually used.

It is easy to find that procedures which reduce a BS equation [Eq. (9)] to an equivalent Lippmann-Schwinger-type equation [Eq. (18)] are exact; however, they are artificial. There are infinite ways to introduce the projection operators (5) and (6). Also, there are many choices to define the three-dimensional Green's function (8). The differences among various types of three-dimensional rel-

ativistic equations, such as (18), are not only reflected in the choice of  $g_E(\xi)$  and the projection of the kernel  $I'$  to  $\hat{T}'$ , but also in the relationship of  $I'$  to the original BS kernel  $I$  [Eq. (12)]. The "goodness" of neglecting the higher term in Eq. (12) is most important for using the three-dimensional equation to replace the BS equation. Apparently, there will be no unique criterion for making the choice of the reduction procedure. It depends very much on the special physical problem and the kinematic region. The formalism adapted here has been widely suggested [8] in various modifications. The primary motivation is that for the low-energy scattering the dominant contribution to the four-point Green's function from the intermediate states with constituent fermions does not vary much from its mass shell. For a bound state, it means that the binding energy is small compared with the constituent quark masses, i.e.,  $(2m - M)/2m \ll 1$ . There-

fore the Green's function  $G_0$  [Eq. (10)] in the BS equation can be replaced by  $G'_0$  [Eq. (7)], which only produces a two-fermion cut in the physical region. In other words, negative spinor space with a large value of the relative energy [ $k^0 \gg (m - M/2)$ ] which characterizes components of an antifermion can be put into a role as higher-order corrections represented by the expansion (12) or just simply can be neglected.

Now the wave function  $\psi_M(\mathbf{q})$  in the three-dimensional space can be defined as

$$\int d^3q' \hat{T}'_M(\mathbf{q}; \mathbf{q}') \psi_M^0(\mathbf{q}') = \int d^3q' \hat{T}'_M(\mathbf{q}; \mathbf{q}') \psi_M(\mathbf{q}'), \quad (19)$$

where  $\psi_M^0(\mathbf{q})$  satisfies the equation

$$[M - H_1(\mathbf{p}) - H_2(-\mathbf{p})] \psi_M^0(\mathbf{p}) = 0. \quad (20)$$

Substituting (18) into (19), we have

$$\psi_M(\mathbf{q}) = \psi_M^0(\mathbf{q}) + \int d^3q' g_M(\mathbf{q}) \hat{T}'_M(\mathbf{q}; \mathbf{q}') \psi_M(\mathbf{q}'), \quad (21)$$

and its integro-differential form is

$$[E - H_1(\mathbf{q}) - H_2(-\mathbf{q})] \psi_M(\mathbf{q}) = \int d^3q' \hat{T}'_M(\mathbf{q}; \mathbf{q}') \psi_M(\mathbf{q}'). \quad (22)$$

Noting the projection operator in (17), the operator on the left-hand side of (22) can be replaced by  $(E - 2E_q)$ . If all the corrections to the BS kernel in Eq. (12) are neglected,  $I' = I$ , and assuming that the BS kernel is a function of only the four-momentum transfer, then we have reached Eqs. (1)–(4) stated at the beginning of this section. One characteristic feature of this equation is that when we assume that the BS kernel is only a function of the four-momentum transfer and is energy independent, the potential in Eq. (3) is also energy independent. As a result, Eq. (1) becomes a completely linear ei-

genvalue problem such as the Schrödinger equation with a Hermitian potential. Consequently, the normalization of the wave function takes the same form as the Schrödinger theory. If we take into account higher-order corrections to the kernel, terms in Eq. (12) beyond the first term, the three-dimensional potential must be energy dependent even though the BS kernel is energy independent. In that case the normalization of the wave function in the nonlinear equation has to follow the same rule for the normalization of the BS wave function as is used usually [13]. Another comment we would like to make is that the relationship between the three-dimensional wave function which is introduced by Eq. (19) and the BS wave function is not clear, at least there is no analytical formalism to connect them. This disadvantage appears in this special reduction approach. For other types of reduction formalism, for example, the one-time relativistic equation [10], it is possible to present explicitly a relation both for the wave function and the scattering amplitude.

Finally, for the quarkonium system, we need to charge conjugate one of the quarks in our identical two-quark system, which amounts to including a matrix  $C$  ( $C^{-1}$ ) on the incoming (outgoing) antiquark side of each vertex where  $C = i\gamma^2\gamma^0$  is the charge-conjugation matrix. However, we will only consider the charge conjugation for one of the quarks (for example, quark 2), both in the incoming and outgoing sides. The reason for excluding another possibility that both incoming (outgoing) quarks charge conjugate to be antiquarks is the following: The color coupling matrix for a quark-gluon vertex is a Gell-Mann matrix, which will vanish on contraction with color-singlet quarkonium states; in other words, quarkonium states cannot directly couple to a single gluon [3]. However, we do not know whether this argument is true or not for the confinement part of the coupling. With these comments we can write down the equation of motion for the quarkonium system as

$$[M - 2E_p] \psi_M(\mathbf{p}) = \sum_j \int d^3q I^j(\Delta^2) [\Lambda_1^+(\mathbf{p}) \beta_1 \Gamma_i^j \Lambda_1^+(\mathbf{q})] \psi_M(\mathbf{q}) [\Lambda_2^-(\mathbf{q}) \beta_2 (\Gamma_2^j)^c \Lambda_2^-(\mathbf{p})]. \quad (23)$$

Here we have used that  $C^{-1} \Lambda^\pm(\mathbf{p}) C = \Lambda^\mp(\mathbf{p})^T$  and  $C \Gamma_i C^{-1} = (\Gamma_i^c)^T$ .  $T$  indicates the transpose operation, and  $\Gamma_i^c$  for the basic  $4 \times 4$  matrix are given by

$$1^c = 1, \quad \gamma_5^c = \gamma_5, \quad \gamma_\mu^c = -\gamma_\mu, \quad (\gamma_\mu \gamma_5)^c = \gamma_\mu \gamma_5, \quad \sigma_{\mu\nu}^c = -\sigma_{\mu\nu}. \quad (24)$$

The wave function  $\psi(\mathbf{q})$  in (23) will be expanded in spinor space with one of them undergoing a charge-conjugate transformation. Details of the representation will be presented in a later section.

### B. Potential

The nonrelativistic potential model has been extensively tested for the pion and up to the  $\epsilon$  with widely used potentials with modifications reflecting various spin structures. The essential feature of the interquark interaction probably can be summarized as a vector-type attractive

Coulomb-like interaction with a damping form factor at short distances plus a scalar-type repulsive linearlike interaction at large distance. The simplest form of the potential can be written as

$$\left[ -\frac{a_c}{r} + a_l r - a_0 \right] e^{-\mu r}, \quad (25)$$

where an exponential factor with  $\mu \rightarrow 0$  has been multiplied to regularize the infrared divergence in the momentum representation. The three-dimensional Fourier transformation of (25) is given by

$$4\pi \left\{ -\frac{a_c}{\mathbf{k}^2 + \mu^2} - \frac{2a_l + 2\mu a_0}{(\mathbf{k}^2 + \mu^2)^2} + \frac{8a_l \mu^2}{(\mathbf{k}^2 + \mu^2)^3} \right\}. \quad (26)$$

With this in mind, we assume the BS kernel of the quark-quark interaction to have the form

$$I(k^2) = I_v(k^2) \sum_i g_i \Gamma_i \otimes \Gamma_i + I_s(k^2) \sum_i c_i \Gamma_i \otimes \Gamma_i, \quad (27)$$

where

$$I_v(k^2) = 4\pi \frac{\alpha_s(k^2)}{k^2 - \mu^2}, \quad (28)$$

$$I_s(k^2) = -4\pi \left\{ \frac{2a_l + 2\mu a_0}{(k^2 - \mu^2)^2} + \frac{8a_l \mu^2}{(k^2 - \mu^2)^3} \right\}, \quad (29)$$

where the index  $i$  in (29) represents  $s, p, v, a,$  and  $t$  corresponding to  $\Gamma_i$  that are  $1, \gamma_5, \gamma_\mu, \gamma_\mu \gamma_5,$  and  $\sigma_{\mu\nu}$ , respectively. The running coupling constant  $\alpha_s(k^2)$  in (28) in the lowest order of QCD has the form [1]

$$\alpha_s(k^2) = \frac{\alpha_s}{\beta \ln(k^2/\Lambda^2)}, \quad k \rightarrow \infty.$$

Here  $\Lambda = \Lambda_{\text{QCD}}$  is the scale parameter of the renormalization-group equation with respect to the subtraction point. However, this form will prevent us from having an analytic expression after the angle integration and will present other computational difficulties. For simplicity, we assume [14]

$$\alpha_s(k^2) = a_c \frac{\Lambda^4}{k^4 + \Lambda^4}, \quad (30)$$

and we still understand this  $\Lambda$  to be  $\Lambda_{\text{QCD}}$ , 100–1000 MeV. Later on, we will find that Eq. (30) will provide a cutoff of the coupling constant in the angle integration, which would not change the analytic behavior of the four-dimensional kernel given by Eqs. (28) and (29) is not a Fourier transformation of any three-dimensional potential, although it duplicates the potential (25) when  $k^0=0$ . Furthermore, the value of  $\mu$  cannot be zero no matter how small it is, since the confinement potential [Eq. (29)] with  $\mu=0$  does not exist. Therefore we have to realize the kernel given by Eqs. (27)–(30) as a distinct model to be compared with the nonrelativistic potential. This model includes three parameters  $a_c, a_1,$  and  $a_0$  plus a QCD scale parameter and an infrared regularizing parameter  $\mu$ , which is supposed to be much smaller than the binding energy of the hadrons,  $\mu \ll (m - M/2)$ . One expects that the solution will not be very sensitive to  $\Lambda$  and  $\mu$ . The ten parameters for describing the spin structures in (27) obviously are redundant. The actual calculations given in the next section show that for the confinement potential most of the parameters have to be set as zero. In brief, we have a kernel with three parameters, and a definite spin structure and a well-behaved analytic property both in the ultraviolet and the infrared region.

### C. Free-spinor representation

In the center-of-mass frame of the quark-antiquark system, a direct product of two free spinors can be arranged in a matrix set:

$$X_H(\mathbf{p}\mu_1\mu_2) = u_H(\mathbf{p}\mu_1) \bar{v}_H(-\mathbf{p}\mu_2), \quad (31)$$

where  $\mathbf{p}$  is the relative momentum,  $\mu_1$  and  $\mu_2$  are the eigenvalues of the helicity operators for the free quark and antiquark, respectively, and the index  $H$  indicates the helicity representation. The definition and the transformation properties of the Dirac spinor are collected in Appendix A. In particular, we are using a normalization of  $u^\dagger u = v^\dagger v = 1$ . Therefore

$$\text{Tr}[X_M^\dagger(\mathbf{p}\mu_1\mu_2) X_M(\mathbf{p}\mu'_1\mu'_2)] = \delta_{\mu_1\mu'_1} \delta_{\mu_2\mu'_2}. \quad (32)$$

In the c.m. frame of the two-particle system, the relative orbital angular momentum is perpendicular to the relative momentum; therefore, the summation of the projection of the spin for two particles along the direction of the relative motion is equal to the projection of the total spin in the same direction. The projection of the total spin of the quark-antiquark system is along the direction of the relative motion,  $\mu = \mu_1 + \mu_2$ , where the plus sign is due to the fact that the spin projection for the negative-energy state is defined along the negative  $z$  axis, thus rotating the negative  $z$  axis to the  $-\mathbf{p}$  direction just like rotating the  $z$  axis to the  $\mathbf{p}$  direction. As a result, the helicity of the quark and antiquark is added to each other, which is opposite to the case of the two-particle system. Although Eq. (31) has a definite value for the projection of the total spin on the direction of relative motion, it does not transform according to an irreducible representation of the three-dimensional rotation group and it can be expanded in terms of the matrix with a definite total spin (see Appendix A):

$$X_H(\mathbf{p}\mu_1\mu_2) = \sum_{JM} \left[ \frac{2J+1}{4\pi} \right]^{1/2} d_{M,J\mu}^J(\theta) X_H(pJM_J\mu_1\mu_2), \quad (33)$$

where  $p = |\mathbf{p}|$  and  $\theta$  is the direction of  $\mathbf{p}$ . The inverse relation of Eq. (33) can be written through the orthogonality relation for the rotation matrices:

$$X_H(pJM_J\mu_1\mu_2) = \left[ \frac{2J+1}{4\pi} \right]^{1/2} \int d\Omega d_{M,J\mu}^J(\theta) X_H(\mathbf{p}\mu_1\mu_2), \quad (34)$$

where  $d\Omega = \sin\theta d\theta d\phi$ .

Now we expand the three-dimensional wave function in terms of the  $X$  tensor (31):

$$\psi_M(\mathbf{p}) = \sum_{\mu_1\mu_2} \psi_M(\mathbf{p}\mu_1\mu_2) X_H(\mathbf{p}\mu_1\mu_2), \quad (35)$$

and

$$\psi_M(\mathbf{p}\mu_1\mu_2) = \text{Tr}[X^\dagger(\mathbf{p}\mu_1\mu_2)\psi_M(\mathbf{p})] . \quad (36)$$

$$(M - 2E_p)\psi_M(\mathbf{p}\mu_1\mu_2) = \sum_{\lambda_1\lambda_2} \int d^3q (\lambda_1\lambda_2 | V(\mathbf{p}, \mathbf{q}) | \mu_1\mu_2) \psi_M(\mathbf{q}\lambda_1\lambda_2) , \quad (37)$$

Substituting Eq. (35) into Eq. (23), we obtain

where

$$\begin{aligned} (\lambda_1\lambda_2 | V(\mathbf{p}, \mathbf{q}) | \mu_1\mu_2) &= \sum_{\alpha} I_{\alpha}(\Delta^2) \text{Tr}\{X^\dagger(\mathbf{p}\mu_1\mu_2)\Lambda_1^+(\mathbf{p})\beta_1\Gamma_{1\alpha}\Lambda_1^+(\mathbf{q})X(\mathbf{q}\lambda_1\lambda_2)\Lambda_2^-(\mathbf{-q})(\Gamma_2^{\alpha})^c\beta_2\Lambda_2^-(\mathbf{-p})\} \\ &= \sum_{\alpha} I_{\alpha}(\Delta^2) \text{Tr}\{\beta_2X^\dagger(\mathbf{p}\mu_1\mu_2)\beta_1\Gamma_{1\alpha}X(\mathbf{q}\lambda_1\lambda_2)(\Gamma_2^{\alpha})^c\} \\ &= \sum_{\alpha} I_{\alpha}(\Delta^2) [\bar{u}(\mathbf{p}\mu_1)\Gamma_{1\alpha}u(\mathbf{q}\lambda_1) \otimes \bar{v}(\mathbf{-q}\lambda_2)(\Gamma_2^{\alpha})^c v(\mathbf{-p}\mu_2)] . \end{aligned} \quad (38)$$

In obtaining the second equality of Eq. (38), we have used the relation

$$\Lambda_1^+(\mathbf{q})X_H(\mathbf{q}\lambda_1\lambda_2)\Lambda_2^-(\mathbf{-q}) = X_H(\mathbf{q}\lambda_1\lambda_2) , \quad (39)$$

and

$$\Lambda_2^-(\mathbf{-p})X_H^+(\mathbf{p}\mu_1\mu_2)\Lambda_1^+(\mathbf{p}) = X_H^+(\mathbf{p}\mu_1\mu_2) . \quad (40)$$

By applying Eq. (33), we are able to carry out the integration with respect to the angle and transform [Eq. (37)] to the representation with a total spin. To do this, we define

$$\psi_M(\mathbf{p}\mu_1\mu_2) = \sum_{JM_J} \left[ \frac{2J+1}{4\pi} \right]^{1/2} d_{M_J\mu}^J(\theta) \psi_M^{JM_J}(\mathbf{p}\mu_1\mu_2) , \quad (41)$$

and

$$\psi_M^{JM_J}(\mathbf{p}\mu_1\mu_2) = \left[ \frac{2J+1}{4\pi} \right]^{1/2} \int d\Omega d_{M_J\mu}^J(\theta) \psi_M(\mathbf{p}\mu_1\mu_2) , \quad (42)$$

where

$$\psi_M^{JM_J}(\mathbf{p}\mu_1\mu_2) = \text{Tr}\{X_H^+(pJM_J\mu_1\mu_2)\psi(\mathbf{p})\} . \quad (43)$$

Substituting Eq. (41) into Eq. (37) and choosing  $\mathbf{p}$  in the direction of the  $z$  axis, we have

$$\begin{aligned} (M - 2E_p)\psi_M^{JM_J}(\mathbf{p}\mu_1\mu_2) &= \sum_{\lambda_1\lambda_2} \int q^2 dq (\lambda_1\lambda_2 | V^J(pq) | \mu_1\mu_2) \psi_M^{JM_J}(q\lambda_1\lambda_2) , \end{aligned} \quad (44)$$

where

$$(\lambda_1\lambda_2 | V^J(pq) | \mu_1\mu_2) = \int d\Omega_q d_{M\lambda}^J(\theta_q) (\lambda_1\lambda_2 | V(\mathbf{p}, \mathbf{q}) | \mu_1\mu_2) , \quad (45)$$

where  $\theta_q$  is the polar angle for  $\mathbf{q}$ . In reaching this equation, we have used  $d_{mM}^J(0) = \delta_{mM}$ .

One of the advantages for setting the equation of motion in the helicity representation is that there is an

extremely simple unitary transformation relating the basis represented by  $\mu_1$  and  $\mu_2$  to the representation with relative orbital angular momentum  $L$  and internal spin  $S$  [17]:

$$X_H(pJM_J\mu_1\mu_2) = \sum_{LS} C_{JM_J}(\mu_1\mu_2; LS) X(pJM_JLS) , \quad (46)$$

$$\begin{aligned} C_{JM_J}(\mu_1\mu_2; LS) &= \left[ \frac{2J+1}{2L+1} \right]^{1/2} \langle L0S\mu | J\mu \rangle \langle \frac{1}{2}\mu_1\frac{1}{2}\mu_2 | S\mu \rangle (-1)^{1/2+\mu_2} . \end{aligned} \quad (47)$$

Equations (46) and (47) are derived in Appendix A. Although the derivation is a little lengthy, the result of Eqs. (46) and (47) is much simpler than if we started with the canonical representation. Let us define

$$\psi_M^{JM_J}(pLS) = \text{Tr}\{X(pJM_JLS)\psi(\mathbf{p})\} . \quad (48)$$

Equation (45) can be written as

$$\begin{aligned} (M - 2E_p)\psi_M^{JM_J}(pLS) &= \sum_{L'S'} \int q^2 dq (L'S' | V^J(pq) | LS) \psi_M^{JM_J}(qL'S') , \end{aligned} \quad (49)$$

where

$$\begin{aligned} (L'S' | V^J(pq) | LS) &= \sum_{\mu_1\mu_2\lambda_1\lambda_2} C_{JM_J}(\lambda_1\lambda_2; L'S') C_{JM_J}(\mu_1\mu_2; LS) \\ &\quad \times (\lambda_1\lambda_2 | V^J(pq) | \mu_1\mu_2) . \end{aligned} \quad (50)$$

Combining Eqs. (17), (27), (38), (45), (47), and (50) and the definition of helicity spinors given in Appendix A, we have calculated all the matrix elements  $(L'S' | V^J(pq) | LS)$  for  $J=0$  and 1, as listed in Appendix B. Now we come to the end of the algebraic derivation. What is left is the numerical work to solve Eq. (49) for the wave function of states with definite  $L$ ,  $S$ , and  $J$ .

#### D. Space and charge parity

The bound states can be classified by the quantum numbers  $L$  and  $S$  only if we can expand the bound-state wave function in terms of free-quark and antiquark spinors. Generally speaking, we cannot restrict the covariant spin structure to only such a free-quark-antiquark system. For the quarkonium system, space and charge parity are the rigorous quantum numbers for classifying its states [12]. In nonrelativistic potential models, it is well known that space and charge parity relate to  $L$  and  $S$  by

$$P = L + 1, \quad (51)$$

$$C = L + S. \quad (52)$$

Let us take a look at how these relations are realized in a covariant free-spinor space. Under the space inversion, according to (A19), the  $X$  tensors transform as

$$\begin{aligned} \not{\epsilon} X_H(\mathbf{p}\mu_1\mu_2)\not{\epsilon}^{-1} &= \not{\epsilon} u(p\mu_1)\bar{v}(-\mathbf{p}\mu_2)\not{\epsilon}^{-1} \\ &= -X_H(-\mathbf{p}-\mu_1-\mu_2). \end{aligned} \quad (53)$$

Under charge conjugation the quarkonium system transforms to itself if we add an interchange operation with a Fermi statistical sign. So the charge parity will be determined by the transformation of the basis under the action of the exchange operator  $-\varepsilon_{12}$  that interchanges the indices of two spinors. It is defined as

$$-\varepsilon_{12} X_H(\mathbf{p}\mu_1\mu_2) = -(-1)^{1-\mu} X_H(-\mathbf{p}-\mu_2-\mu_1). \quad (54)$$

The meaning of this transformation can be explained in two aspects. (i) The spin projection in the helicity representation has the same value as the spinor in the rest frame (see Appendix A), and the  $z$  axis for defining the spin projection is opposite for the positive- and the negative-energy spinors. Therefore, when the index  $\mu_2$  ( $\mu_1$ ) is exchanged to positive (negative) spinors, one must flip their sign at the same time. (ii) Exchanging the indices also includes a reversal of the relative momentum in each spinor. However, we cannot just simply let  $\mathbf{p}$  go to  $-\mathbf{p}$  and vice versa. In the helicity representation, the phase of the spinors is fixed independently for  $\mathbf{p}$  and  $-\mathbf{p}$ . Therefore, when we flip the direction of  $\mathbf{p}$ , a phase difference has to be counted precisely. The phase  $(-1)^{1-\mu}$  in Eq. (54) is the phase difference in the definition of spinors for the positive and negative directions of the momentum (A1)–(A4).

Combining Eqs. (33), (46), and (47), we have

$$X_H(\mathbf{p}\mu_1\mu_2) = \sum_{JM_JLS} A_{JM_JLS}(\theta\mu_1\mu_2) X(pJM_JLS), \quad (55)$$

where

$$\begin{aligned} A_{JM_JLS}(\theta\mu_1\mu_2) &= \frac{2J+1}{\sqrt{4\pi(2L+1)}} \langle LOS\mu | J\mu \rangle \\ &\times \langle \frac{1}{2}\mu_1 \frac{1}{2}\mu_2 | S\mu \rangle (-1)^{1/2+\mu_2} d_{M_J,\mu}^J(\theta). \end{aligned} \quad (56)$$

To expand the right-hand side of Eq. (53), according to

Eq. (55), we get

$$\begin{aligned} -X_H(-\mathbf{p}-\mu_1-\mu_2) &= - \sum_{JM_JLS} (-1)^{1+\mu_1-\mu_2} A_{JM_JLS}(\theta+\pi-\mu_1-\mu_2) \\ &\times X(pJM_JLS), \end{aligned} \quad (57)$$

where the phase is given by  $(-1)^{1+\mu_1-\mu_2}$  again since the direction of  $-\mathbf{p}$  on the left-hand side is defined not just by changing  $\theta \rightarrow \theta + \pi$ , but by the extra phase given by (A1)–(A4). By using the symmetry properties of  $3j$  symbols and the rotation functions, it is easy to show from (56) that

$$\begin{aligned} (-1)^{\mu_1-\mu_2} A_{JM_JLS}(\theta+\pi-\mu_1-\mu_2) &= (-1)^{1+L} A_{JM_JLS}(\theta\mu_1\mu_2). \end{aligned} \quad (58)$$

Combining (53), (55), (57), and (58), we have

$$\not{\epsilon} X(pJM_JLS)\not{\epsilon}^{-1} = (-1)^{1+L} X(pJM_JLS). \quad (59)$$

By the same token, the right-hand side of Eq. (54) is given as

$$\begin{aligned} (-1)^\mu X_H(-\mathbf{p}-\mu_2-\mu_1) &= \sum_{JM_JLS} A_{JM_JLS}(\theta+\pi-\mu_2-\mu_1) X(pJM_JLS). \end{aligned} \quad (60)$$

From Eq. (56) we have

$$A_{JM_JLS}(\theta+\pi-\mu_2-\mu_1) = (-1)^{L+S} A_{JM_JLS}(\theta\mu_1\mu_2) \quad (61)$$

and

$$-\varepsilon_{12} X(pJM_JLS) = (-1)^{L+S} X(pJM_JLS). \quad (62)$$

Equations (59) and (62) demonstrate that the basis of free covariant spinors in the c.m. frame of the quarkonium system with the quantum numbers  $J$ ,  $L$ , and  $S$  possesses the same space and charge parity as that given by Eqs. (51) and (52).

### III. RESULTS

The aim of this section is to find the low-lying eigenvalues of Eq. (49) with the potential given in Appendix B. The numerical integration is performed by mapping the magnitude of momentum,  $q$ , onto a finite interval. In our calculation we have used

$$q = \xi \tan \pi x / 2, \quad x \in [0, 1], \quad (63)$$

where  $\xi$  is a constant scale parameter. For simplicity, the interval is partitioned into  $N$  equal-length steps and a trapezoidal rule has been used. In several cases we have tried Gaussian quadrature to evaluate the integral equation, but no qualitative difference is found. The key issue of this numerical calculation is to find out the consistency of the physical model. The numerical accuracy will make sense after we understand the general behavior of this model, and therefore we prefer to use a simple numerical method to study Eq. (49) at this stage. Now the integral

equation (49) is transformed to an eigensystem of linear equations of order  $N$  for the case of  $J^{PC}=0^{-+}, 1^{+-}, 0^{++}$ , and  $1^{++}$  and of order  $2N$  for the case of  $J^{PC}=1^{-}$ . The transformation scaling factor  $\xi$  will be fixed by minimizing the lowest eigenvalue of bound states  $J^{PC}$  for each set of points  $N$ .  $\xi$  does not vary significantly for different  $J^{PC}$ . However, it increases rapidly with  $N$ . Now let us describe the main results of solving the integral equation (49) to obtain eigenvalues and wave functions of the low-lying states.

#### A. Bound states embedded in the spurious continuums

The major difference between Eq. (49) and the Schrödinger equation with the linear potential is that, in addition to bound states, continuum states can also be solutions of (49). This is due to the fact that the height of the potential in the equation of motion in momentum space is finite. In the Schrödinger equation with the linear potential, which can be infinitely high, only well-separated bound states are solutions. Unlike this case, the potential with the well-behaved property in the infrared regime in momentum space does not lead to adequate confinement. Whenever the infrared regularization

parameter  $\mu$  (however small) is used, the potential provides a barrier with a finite height. As a result, the continuum states are also solutions of Eq. (49) as long as the eigenvalue is larger than twice the mass of the constituent quark. These states do not have any physical meaning. Their existence is due to a complete lack of an ansatz to describe absolute confinement in the momentum space. So we call it the "spurious continuum" since it is caused by the approximation scheme. Assuming that the charm quark has a mass of  $\sim 1.64$  GeV, most of the charmonium states except  $\eta_c$  (2.980) and  $J/\psi$  (3.096) are higher than the mass of two free charm quarks. In other words, most of the charmonium states are embedded in the spurious continuum. For the  $b\bar{b}$  system, except for the ground state, all of the excited states have a similar feature. Therefore the first task in working with this model is to identify bound states in the spurious continuum. Actually, the identification of an eigenvalue (bound state) is quite unique: by counting the nodes of the corresponding eigenfunction. In Table I the first 30 states have been listed for the system  $\eta_c$  with  $J=L=S=0$ . In the case of  $N=60$ , the states with 0,1,2,3,... nodes are buried, in order, in the continuum states, i.e., states with a large number of nodes. When the number of points is increased to 100 and 150, more and more states with

TABLE I. First 30 states for  $\eta_c$  system with  $J=L=S=0$ .

	$N=60, \xi=0.914$ GeV		$N=100, \xi=1.160$ GeV		$N=150, \xi=1.400$ GeV	
	Eigenvalue (MeV)	No. of nodes	Eigenvalue (MeV)	No. of nodes	Eigenvalue (MeV)	No. of nodes
1	3055	0	3041	0	3040	0
2	3389	31	3303	27	3286	43
3	3428	30	3317	28	3292	27
4	3471	31	3332	28	3299	28
5	3517	41	3348	29	3306	54
6	3567	31	3365	35	3314	34
7	3621	29	3384	30	3323	68
8	3631	1	3404	42	3333	33
9	3678	30	3425	32	3343	29
10	3740	31	3447	33	3354	30
11	3804	31	3471	34	3365	29
12	3872	30	3495	39	3377	38
13	3942	29	3521	33	3389	32
14	4015	28	3549	33	3402	40
15	4029	2	3577	35	3416	34
16	4090	28	3594	1	3430	35
17	4167	28	3607	35	3444	32
18	4245	26	3639	35	3459	43
19	4321	3	3671	35	3475	35
20	4324	26	3705	35	3491	33
21	4403	25	3741	35	3508	33
22	4480	24	3777	37	3526	38
23	4537	4	3815	36	3544	34
24	4556	21	3855	36	3562	34
25	4629	19	3895	39	3582	34
26	4690	5	3937	40	3593	1
27	4697	16	3974	2	3601	37
28	4756	14	3980	35	3621	47
29	4782	8	4025	50	3642	46
30	4808	13	4070	41	3664	38

redundant nodes are embedded between the ground state and the state with one node. So these high-node states without any stability appear for various grid sizes and their position changes rapidly. On the other hand, comparing the eigenvalue of the ground state and the state with one node in the case of  $N=100$  and 150, one finds that they are absolutely stable. Thus we find that the method of counting the number of nodes in the eigenfunction provides us an identification of bound states without confusion. One more example of the  $J/\psi$  system is given in Table II. There are two components corresponding to  $JLS=101$  and 121 coupled together in Eq. (49). We have to count the nodes for both components, say,  $(n_S, n_D)$ . In Table II we have omitted a large number of these meaningless continuum states, but kept the ones that appear in the region where the bound states are embedded. It is clearly shown that the first and second excited states with nodes (1,2) and (2,2) buried in the continuums have almost the same eigenvalue in the cases of  $N=100$  and 150. In these two examples, the lowest eigenvalue which is below the value of  $2m_c$  is a bound state. For the other cases such as  $J^{PC}=1^{+-}$ ,  $0^{++}$ , and  $1^{++}$ , even the lowest eigenvalue is embedded in the middle of a host of continuum states.

In the above calculation, the scaling parameter  $\xi$  is

fixed by minimizing the lowest eigenvalue among bound states as mentioned earlier. The spin parameters have been chosen to be 1 for  $c_s$  and  $g_v$  and 0 for all the others. In other words, only the scalar confinement and vector Coulomb parts have been considered. The detailed role of other parameters will be discussed in the following subsection.

### B. General features of the parameters

Since there are so many parameters involved, it is better to have a general idea about these parameters before we use this model to fit the experimental data. The purpose of this numerical calculation is to study the characteristics of the equation itself. Therefore the parameters adopted here will rely a great deal on the experience provided by previous works [1–3].

There is not much ambiguity for the quark-mass parameters  $m_c=1.64$  GeV and  $m_b=5$  GeV. It has been checked that the solutions of the equation are highly insensitive to the parameter of the ultraviolet cutoff for the Coulomb potential,  $\Lambda_{\text{QCD}}$ . There is no significant difference that can be found when  $\Lambda_{\text{QCD}}$  varies from 200 to 800 MeV. We have fixed  $\Lambda_{\text{QCD}}$  to be 800 MeV. The most sensitive parameter in this model is  $\mu$ , the one for

TABLE II. Example of  $J/\psi$  system.

	$N=100, \xi=1.160$ GeV			$N=150, \xi=1.400$ GeV		
	Eigenvalue (MeV)	No. of nodes in $S$ wave	No. of nodes in $D$ wave	Eigenvalue (MeV)	No. of nodes in $S$ wave	No. of nodes in $D$ wave
1	3041	0	0	3041	0	0
2	3286	0	15	3280	0	13
3	3303	9	19	3286	25	41
4	3303	24	19	3286	0	15
5	3317	25	19	3292	25	27
28	3549	22	29	3402	20	25
29	3577	31	29	3415	29	25
30	3578	22	29	3416	20	25
31	3595	1	2	3430	29	25
32	3607	32	28	3430	20	25
33	3608	21	28	3444	31	25
34	3639	32	27	3445	22	25
35	3639	23	27	3459	31	27
36	3645	2	2	3460	22	27
37	3671	34	28	3475	31	27
38	3672	25	28	3476	22	27
39	3705	34	30	3491	31	27
48	3855	28	30	3563	24	29
49	3895	35	30	3582	31	29
50	3896	28	30	3582	24	29
51	3937	35	30	3593	1	2
52	3938	28	30	3601	32	28
53	3975	2	1	3602	23	28
54	3980	35	30	3622	32	29
55	3981	28	30	3622	25	29
56	4006	3	2	3642	34	27
57	4024	36	29	3643	27	27
58	4025	29	29	3644	2	2
59	4069	35	29	3664	32	32
60	4070	28	29	3664	25	28

regularizing infrared behavior, particularly in the confinement part of the potential. (For the Coulomb part, this regularization is not necessary.) The variation of  $\mu$  could cause a rapid change of the solution, which means that  $\mu$  characterizes a steep variation of the confinement potential in the infrared regime. As a result,  $\mu$  becomes a sensitive parameter for the eigensystem. However, there exists a kind of convergent picture if we increased the grid points  $N$  when  $\mu$  is reduced. Therefore it depends very much on the capacity of the computer. In this work we have fixed  $\mu=50$  MeV. A trial with a smaller value of  $\mu$  will lead to a very large eigensystem if consistent results are to be produced.

The potential parameters  $a_c$ ,  $a_l$ , and  $a_0$  will be chosen for duplicating the model in the Schrödinger formalism so that  $a_c=0.272$ ,  $a_l=0.25$  GeV<sup>2</sup>, and  $a_0=1$  GeV [1–3]. Any small adjustment of these parameters will be justified in the course of the calculations. The set of parameters stated above has been used in obtaining Tables I and II. Now we turn to the spin parameters. The five parameters for modifying the confinement potential are indicated by  $c_s$ ,  $c_v$ ,  $c_a$ ,  $c_p$ , and  $c_t$ . We find that the mass spectroscopy of  $\eta_c$  and  $J/\psi$  does not change significantly when we vary the combination  $(c_s, c_v)=(0, 1)$ ,  $(1, 0)$ , and  $(0.5, 0.5)$ . Therefore it is reasonable to describe the spin structure of the confinement potential by taking a scalar interaction plus certain components of the vector term. This is consistent with the assumption made in Ref. [1]. However, any small admixture of the axial-vector, pseudoscalar, and tensor components will completely destroy the spectrum of the  $J/\psi$  system. Even the lowest eigenvalues of  $J/\psi$  and  $\eta_c$  are totally unacceptable even for a small value of  $c_a$ ,  $c_t$ , and  $c_p$ . Therefore an assumption must be made that this kind of confinement potential does not involve any spin component arising from the pseudoscalar, axial-vector, and tensor components. For simplicity, the  $c$  parameter set is  $c_s=1$ ,  $c_p=c_t=c_a=c_v=0$ ; i.e., only the scalar type of confinement potential has been considered.

The modification of the spin structures characterized by  $g_s$ ,  $g_p$ ,  $g_v$ ,  $g_a$ , and  $g_t$  to the Coulomb part of the potential appears quite different. When we change each of these parameters individually, the mass spectroscopy varies smoothly in a very similar pattern within a reasonable range. Therefore the main task in obtaining the mass spectroscopy of the quarkonium system is to determine this set of parameters. There are two significant features of the solution in terms of the variation of these five parameters: (a) Whenever we change the parameters  $g_v$  and  $g_s$  by any reasonable value, the ground state of  $\eta_c$  of  $J/\psi$  remain stubbornly degenerate, as shown in Tables I and II. In other words, the scalar and vector (even including pseudoscalar) terms do not provide any significant spin-spin interaction, in the terminology of the nonrelativistic description. In order to have an appropriate separation between the two lowest states  $0^{-+}$  and  $1^{--}$  (or  $^1S_0$  and  $^3S_1+^3D_1$ ), one has to include a certain amount of the axial-vector and tensor interaction components in the Coulomb part of the potential. (b) The variation of the pseudoscalar parameter  $g_p$  seems to have no effect on any eigenvalues.

These two general features are probably the most important reasons that account for the great success of the nonrelativistic approach. Since the wave functions of bound states must decrease rapidly in the region of high momenta, the eigenvalues of Eq. (49) are determined by the part of the kernel with relatively small momentum components. If we drop all the terms which are proportional to  $B_p$  in the kernel given by Appendix B, as one usually does in the nonrelativistic approximation where  $B_p=|\mathbf{p}|/(E_p+m)\ll 1$  when  $|\mathbf{p}|$  is small, the asymptotic part of the kernel in the region with small  $p$  looks like

$$(00|V_0(pq)|00)\sim r_s(1)+r_v(1)-r_a(1)+r_t(1), \quad (64)$$

$$(01|V_1(pq)|01)\sim r_s(1)+r_v(1)+r_a(1)-r_t(1), \quad (65)$$

$$(21|V_1(pq)|21)\sim -\frac{1}{2}r_s(1)-\frac{1}{2}r_v(1)+\frac{7}{6}r_a(1)-\frac{7}{6}r_t(1) \\ +\frac{3}{2}[r_s(3)+r_v(3)-r_a(3)+3r_t(3)], \quad (66)$$

$$(01|V_1(pq)|01)\sim \frac{2\sqrt{2}}{3}[r_a(1)-r_t(1)], \quad (67)$$

$$(11|V_0(pq)|11)\sim r_s(2)+r_v(2)-r_a(2)+r_t(2), \quad (68)$$

$$(10|V_1(pq)|10)\sim r_s(2)+r_v(2)-r_a(2)+r_t(2), \quad (69)$$

$$(11|V_1(pq)|11)\sim r_s(2)+r_v(2)+r_a(2)-r_t(2), \quad (70)$$

where  $r_i(n)$  are defined by (B9)–(B13). They represent parameters of the corresponding spin structure multiplying the angle integrals, which are well defined both in the ultraviolet and infrared region and vary smoothly with the momentum variable. From (64) and (65), we can immediately find that the differences of the potential for the  $\eta_c$  and  $S$  components of  $J/\psi$ , corresponding to  $JLS=000$  and  $101$ , are only those that appear from the axial-vector and tensor components; the scalar and vector components are completely the same. Therefore the spin-spin interaction in the nonrelativistic terminology cannot be provided only by vector and scalar bilinear covariants. The source of the spin-spin interaction is mainly due to the axial-vector and tensor components. Furthermore, from (67), the coupling potential, which would be called the tensor interaction in the nonrelativistic regime, between  $S$  and  $D$  components of the  $J/\psi$  system also arises from the same source. In other words, both the spin-spin and tensor forces in the nonrelativistic theory should be derived from the axial-vector and tensor-bilinear covariants. Finally, among all of the expressions of (64)–(70), the pseudoscalar component never appears, and so the  $\gamma_5\otimes\gamma_5$  term never plays a significant role. A brief summary for the spin parameters in the Coulomb part of the potential is that the scalar and vector terms have very similar property for all states, the axial-vector and tensor components are absolutely important in determining the spectra of quarkonium systems, and the pseudoscalar term can be neglected in bound-state problems.

### C. Mass spectroscopy of quarkonium systems

The mass and potential parameters as analyzed in the last subsection are given in Table III. The spin param-

TABLE III. Mass and potential parameters.

$m_c = 1640$ MeV
$\mu = 50$ MeV
$\Lambda_{\text{QCD}} = 800$ MeV
$a_c = 0.272$
$a_t = 0.25 \times 10^6$ MeV <sup>2</sup>
$a_0 = 780$ MeV

ters are given in Table IV, where five sets of the combination of  $g_s$ ,  $g_v$ ,  $g_a$ , and  $g_t$  are suggested. As we mentioned earlier, the parameters  $g_s$  and  $g_v$  play a similar role and  $g_a$  and  $g_t$  are essential for determining the spin structure. So sets 1 and 2 are chosen by combining  $g_v$  and  $g_t$  or  $g_a$ , respectively. Sets 3 and 4 have a similar combination obtained by replacing  $g_v$  with  $g_s$ . In terms of the spectra only, we really do not have too much reason to search for more complicated mixing parameters since there are many different possibilities which could reproduce the spectra by specially fitting certain states and not so well to others. However, to ascertain a variation of the combination, we give a parameter set 5, which gives better results for the first and second excited states of  $J/\psi$ . It is quite a difficult numerical work. So many parameters are involved in such a highly nonlinear problem that involves diagonalizing five matrices at the same time. Particularly, in order to find the eigenvalues, one must calculate the eigenfunctions for identifying the bound states embedded in the spurious continuum.

The results are given in Table V. The first column gives the experimental data as taken from the Particle Data Group [19]. The data for  $h_c(3510)$  are taken from [20], but the evidence is not overwhelming. In the calculation of the eigenvalues as well as in obtaining the wave function of the eigenstates (next section), the number of integration points ( $N$ ) is chosen to be 150 and the trigonometry scale parameter is  $\xi = 1.412$  GeV, which minimize the mass of  $\eta_c$  and  $J/\psi$ . The results provide a qualitative fit to the experimental spectra by various parameter sets. We cannot draw any meaningful dynamical conclusions by using so many parameters to fit the data on the energy of charmonium states, while ignoring completely the experimental database on the electromagnetic and weak transition rates. However, we do learn an important message about the relationship between the Schrödinger formalism and the three-dimensional relativistic approach for studying meson spectroscopy. We can assume that the starting point of the two approaches is the same because both procedures are starting from an

TABLE IV. Spin parameters  $c_s = 1$ ,  $c_p = c_v = c_a = c_t = 0$ , and  $g_p = 0$ .

	$g_s$	$g_v$	$g_a$	$g_t$
Set 1	0	1.89	0	0.985
Set 2	0	1.86	-0.73	0
Set 3	2.49	0	0	1.01
Set 4	2.45	0	-0.776	0
Set 5	1.87	0.49	0.76	2.00

on-shell Feynman diagram as the kernel of a nonperturbative calculation. There are mainly three approximations being made to reduce the nonperturbative problem to a Schrödinger equation within Pauli space in nonrelativistic approach.

(a) The first approximation is a kinematical one, that a nonrelativistic expansion has been carried out for the kinetic energy of a free particle,  $E_p$ . In configuration space this approximation immediately leads to a differential equation. However, for a bound-state problem, the momentum of the constituent quark would not reach very high values in terms of the scale of the heavy quark mass. In addition, a numerical accuracy for treating a differential equation is much better than solving an integral equation. Therefore we do not believe that there would be too much advantage to replacing a differential equation by an integral equation as we have done in the three-dimensional relativistic approach.

(b) In order to write a differential equation in configuration space, a static or instantaneous approximation has to be made in the on-mass-shell kernel. This approximation misses a pole singularity in the light cone. But in our treatment this light-cone pole singularity has been regularized by introducing a small mass  $\mu$ . So there is still no significant difference between the two approaches in this aspect. For example, for the spin-spin force, the static approximation is to move the  $\delta$  singularity from the light cone to the space origin. One cannot expect to make much of a mistake by this approximation. As to the region away from the light cone, whenever a Yukawa function or a Bessel function [21] is taken as the kernel of equation, it would not make a big difference.

(c) Now we come to the third approximation which causes a major difference between the two approaches. All of the spin-dependent forces in the Schrödinger formalism are produced from the small components of the Dirac spinors. In order to make a Fourier transformation of these terms to configuration space, one has to make an approximation that

$$\frac{p}{E_p + m} \sim \frac{p}{2m} \quad (71)$$

This approximation is reasonable for calculating an independent matrix element with small momentum. However, using this approximation in the off-shell kernel would greatly overestimate the importance of the spin-dependent forces. It is clear that the factor on the left-hand side of Eq. (71), which is always smaller than 1, can never be important in all regions of the momentum, unlike the right-hand side of Eq. (71), which can be significant up to certain finite values of the momentum. Furthermore, in the case of bound states, high-momentum configurations are automatically suppressed which reduce the effect of the factor  $p/(E_p + m)$  in the potential. It is hard to produce considerable corrections with such small numbers. Actually, this fact has been repeatedly emphasized in the Wise-Isgur symmetry during recent years [22]. On the other hand, when a factor on the right-hand side of (71) is used, it can produce a considerable effect in the region with a finite but large momentum. As we mentioned in the previous subsection,

TABLE V. Spectra of  $c\bar{c}$  system.

Name	$J^{PC}$	Set 1	Set 2	Set 3	Set 4	Set 5
$\eta_c(2980)$	$0^{-+}$	2980	2980	2980	2908	2980
$\eta_c(3591)$	$0^{-+}$	3588	3570	3630	3614	3634
$J/\psi(3096)$	$1^{--}$	3096	3096	3096	3096	3096
$\psi(3686)$	$1^{--}$	3728	3728	3628	3674	3684
$\psi(3770)$	$1^{--}$	4029	3737	3787	3790	3771
$\psi(4040)$	$1^{--}$	4090	4008	4078	4061	4074
$\psi(4159)$	$1^{--}$	4314	4106	4143	4155	4121
$\psi(4415)$	$1^{--}$	4395	4295	4360	4344	4356
$\chi_0(3415)$	$0^{++}$	3359	3343	3402	3388	3403
$\chi_1(3510)$	$1^{++}$	3483	3506	3522	3542	3489
$h_c(3510)$	$1^{+-}$	3340	3328	3367	3357	3369

the pseudoscalar interaction does not produce any observable effect because the potential related to the pseudoscalar term is proportional to the factor  $B_p$  (see Appendix B). The spin-spin force which is supposed to separate  $\eta_c$  and  $J/\psi$  cannot be produced by a vector or scalar component since the difference of the potential for  $\eta_c$  and the  $L=0$  state of  $J/\psi$  is proportional to  $B_p^2 B_q^2$  [see (B1) and (B5)], and it can be neglected since it is small. Furthermore, the tensor force which leads to a mixing between  $S$  and  $D$  components of the  $J/\psi$  system cannot get this effect from the vector and scalar components [see (B7)]. It is quite an ironic result. In the Schrödinger formalism, the spin-dependent force is considered as a type of relativistic correction. However, the relativistic corrections would disappear or, at least, would become small when one does a relativistic calculation. In order to provide an appropriate spin-dependent force in the three-dimensional relativistic approach, we must put in certain spin structures in the BS kernel in the first place, i.e., to mix certain axial-vector and tensor components in the Coulomb part of the potential. It is obvious that the spin-spin interaction produced by the vector-bilinear covariant is related to the small component of the Dirac spinor, i.e., proportional to  $B_p$ , but the same interaction produced by the axial-vector and tensor-bilinear covariants is related to the large component of the Dirac spinor and is of order 1. It is interesting to note that the strength of the  $S$  and  $D$  components of the wave function is determined by  $g_s$  and  $g_v$  and is large [(B5) and (B6)]. The coupling potential between  $S$  and  $D$  components in the  $J/\psi$  system is dominated by  $g_a$  and  $g_t$  [Eq. (B7)]. Therefore, if only the vector potentials were considered, the tensor force would be extraordinarily small. In other words, one cannot expect too much coupling between  $S$  and  $D$  components with only the vector coupling. The mixing of the  $D$  component in the excited states of the charmonium system is considered in studies of electromagnetic transitions [23]. This problem could shed light on the relationship of the two nonperturbative approaches.

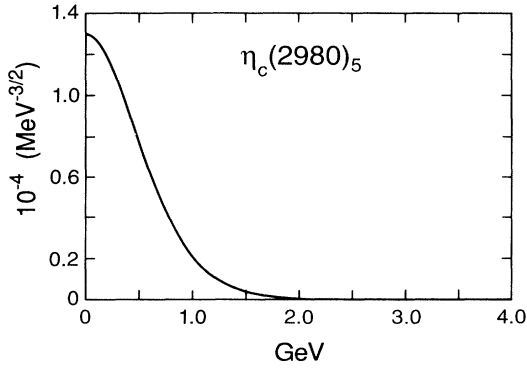
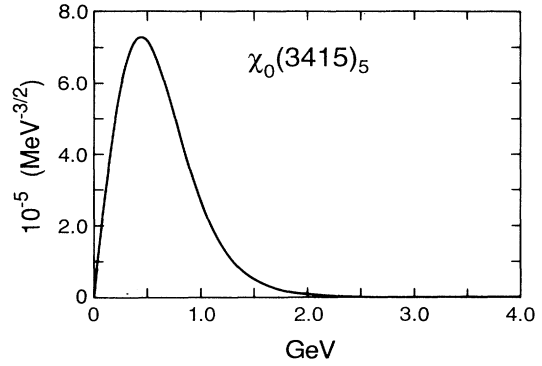
In summary, the nonrelativistic approximation can be phrased simply: The square root factor of  $E_p$  should be replaced by  $m$  or a first-order expansion whenever it appears. In the kinetic term and the gluon propagator, this substitution is acceptable. In the small components of

the Dirac spinors, this substitution exaggerates the spin-dependent forces and this effect will be significantly suppressed in the three-dimensional relativistic approach. As a result, the spin-dependent forces have a completely different origin in these two approaches. In the Schrödinger formalism, it belongs to the higher-order relativistic correction. In the three-dimensional relativistic approach, it should be assumed that the BS kernel is composed of a complicated mixture of the Dirac bilinear covariants in the first place. We are not intending to create an impression that the Schrödinger approach has anything “wrong” since both approaches are entirely phenomenological. Although the spin-dependent force is exaggerated as a result of the nonrelativistic approximation, this approach is simple, powerful, and, more importantly, successful for classifying a great deal of the experimental data. However, the different physical origin of the spin-dependent force does raise a very interesting question for a future study of the meson spectroscopy.

A final remark should be made about the  $b\bar{b}$  system. We have not given the numerical results of the  $b\bar{b}$  system here for the following reasons. First, for such a heavy quark mass, the contributions to the equation are spread over a large momentum region. As a result, we have to increase the number of integration points so that the large momentum region can be covered accurately. Second, from the theoretical point of view and from experience with the calculated results, the spectra of the  $b\bar{b}$  system must possess very similar pattern as the  $c\bar{c}$  system. This is confirmed by observing the experimental data, with the exception of one phenomenon. In the  $J/\psi$  system, the excited states appear as pair of states close together such as  $\psi(3686)$  and  $\psi(3770)$  that are far away from the next pair  $\psi(4040)$  and  $\psi(4159)$ . However, in the  $\Upsilon$  system the experiment does not show any neighboring state around  $\Upsilon(10023)$ , as the coupled equation between  $S$  and  $D$  waves frequently predicts. In any case, it is necessary to treat the  $b\bar{b}$  system more carefully and the results are planned to be presented in a separate paper.

#### D. Wave functions

The wave functions of  $\eta_c$ ,  $\eta_c'$ ,  $\chi_0$ , and  $J/\psi$  are plotted in Figs. 1–4. The results are obtained by using parameter set 5, which has been indicated as a lower index under

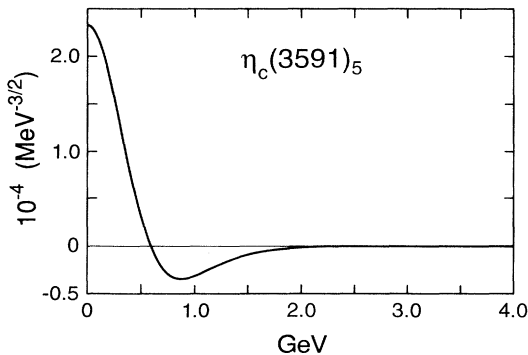
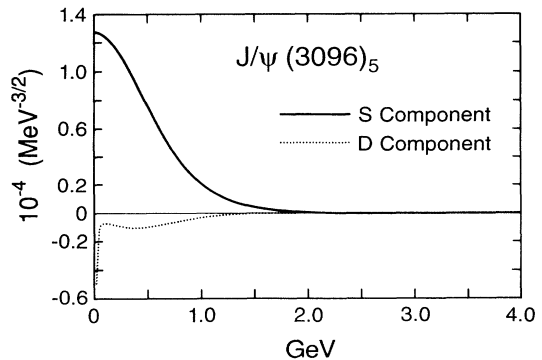
FIG. 1. Wave function of  $\eta_c(2980)$  for parameter set 5.FIG. 3. Wave function of  $\chi_0(3415)$  for parameter set 5.

each particle name. The general shape and number of nodes do not change when we vary from one parameter set to another. The wave functions of  $\chi_1$  and  $h_c$  have very similar pattern as  $\chi_0$  with a small numerical change of the height and center of the lump. The dashed line in Fig. 4 represents the  $D$  component in  $J/\psi$  and can really be neglected. So  $J/\psi$  is a purely  $1S$  state without problem. However, things become very different when we go to the excited states of  $J/\psi$ . Five excited states of the  $J/\psi$  particle are shown in Figs. 5–9, where the solid and dashed lines represent the  $S$  and  $D$  components, respectively. Each of these figures includes three graphs (a), (b), and (c), corresponding to parameter sets 1, 2, and 5, respectively. One can immediately find that the pattern of the  $D$  wave coupled to the  $S$  wave is very sensitive to different parameter sets. In Figs. 6 and 8, which correspond to the states  $\psi(3770)$  and  $\psi(4159)$ , the principal quantum number or nodes of the  $S$  wave can be changed with different parameter sets. The fluctuation of the curves apparently is a numerical problem caused by the kernel given by (B11) within the region of the small momenta where one has to face a numerical uncertainty. Since the diagonal matrix elements of the  $D$  state are much larger than those for the  $S$  state, the corresponding eigenfunctions will fluctuate easily under a variation of the large matrix elements.

In terms of parameter set 5, we can identify  $\psi$  particles in the following way:  $\psi(3686)$  is the  $2S$  state with small mixture of the  $1D$  state,  $\psi(3770)$  is a  $1D$  state with certain mixture of the  $2S$  state,  $\psi(4040)$  is a  $3S-2D$  mixing state,  $\psi(4159)$  is a  $4S$  state, and  $\psi(4415)$  is a  $4S-3D$  mixing state. However, in this description the explicit mixing of states is highly sensitive to the axial-vector and tensor components in the kernel. It is well known that the transition rates are highly sensitive to the wave functions. It will be a useful exercise to consider the energy-level scheme as well as weak and electromagnetic transition rates. This would permit us to make a definite choice of the covariant components that provide the spin structure. Such calculations are in progress. Results would help us to understand the nature and structure of  $J/\psi$  and the excited states. So the three-dimensional relativistic equation with a different spin structure of the bilinear covariants provides a very powerful tool to classify the complete experimental data including the transition rates.

#### IV. SUMMARY

In this paper we have concentrated on the development of an algorithm describing the quarkonium states in terms of a three-dimensional relativistic equation with a covariant spinor structure. This method mainly includes

FIG. 2. Wave function of  $\eta_c(3591)$  for parameter set 5.FIG. 4. Wave function of  $J/\psi(3096)$  for parameter set 5.

four steps. In step 1, a four-dimensional BS kernel, including the Coulomb part with a high-momentum cutoff, a confinement part with a light-cone regularization, and both associated with a complete set of Lorentz covariants, is proposed [Eqs. (17)–(29)]. In step 2, the phenomenological BS kernel is projected onto a three-dimensional space with each fermion being on the mass shell in both incoming and outgoing channels [Eq. (14)]. By using the three-dimensional kernel, the equation of motion for the quarkonium system is given by (23). Step 3 is to expand the wave function in terms of the tensor composed of free Dirac spinors in the helicity representation and  $L$ - $S$  representation. This expansion has been proved in Appendix A. Using this expansion, the equation of motion can be written in the corresponding representation and the angle integration can be carried out analytically as given in Appendix B. Finally, in step 4, the integral equations in one variable, which is the magnitude of the momentum, are studied in detail by a numerical method.

The potential barrier within the equation of motion in momentum space is not infinitely high. As a result, most

of the excited quarkonium states are embedded in a spurious continuum, a property caused by the approximation of the potential with a finite height. By using the method of counting the nodes of the eigenfunction, the bound states can be identified. By changing the number of integration points, the energy of the bound states does not change much, even though the background continuum states are shifted dramatically.

The two mass parameters, quark mass and  $\Lambda_{\text{QCD}}$ , are fixed without much ambiguity. The infrared treatment for the Coulomb part can be performed in a more sophisticated manner in the future, but the  $\mu$  parameter for regularizing the infrared behavior of the confinement potential has a certain inherent ambiguity. The three potential constants  $a_c$ ,  $a_1$ , and  $a_0$  are chosen to be consistent with the nonrelativistic phenomenology. Only the scalar spin structure in the confinement potential has been considered. A set of scalar, vector, axial-vector, and tensor mixing parameters in the Coulomb potential is given for fitting the mass spectroscopy of the quarkonium system.

It is hard to draw any definite dynamical conclusion for this equation unless one can fit the complete experi-

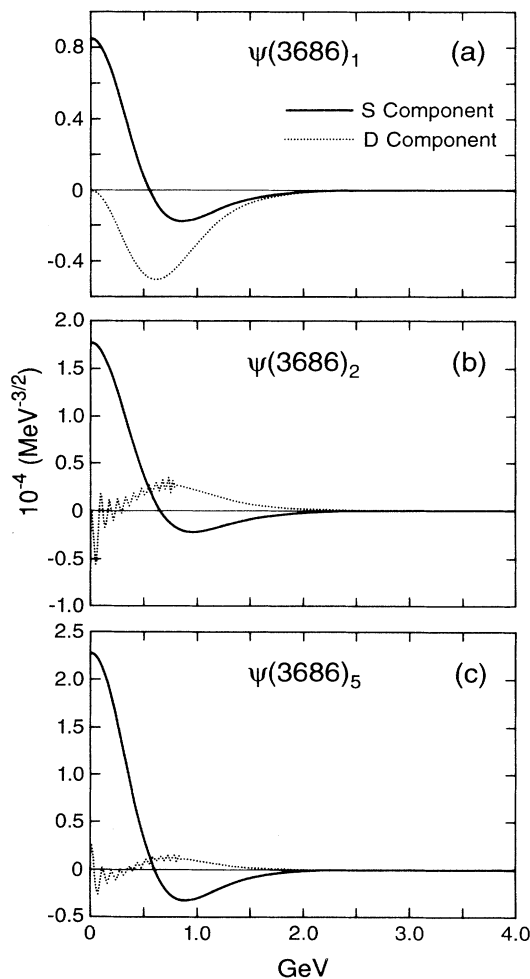


FIG. 5. Wave function of  $\psi(3686)$  for parameter sets (a)1, (b)2, and (c)5.

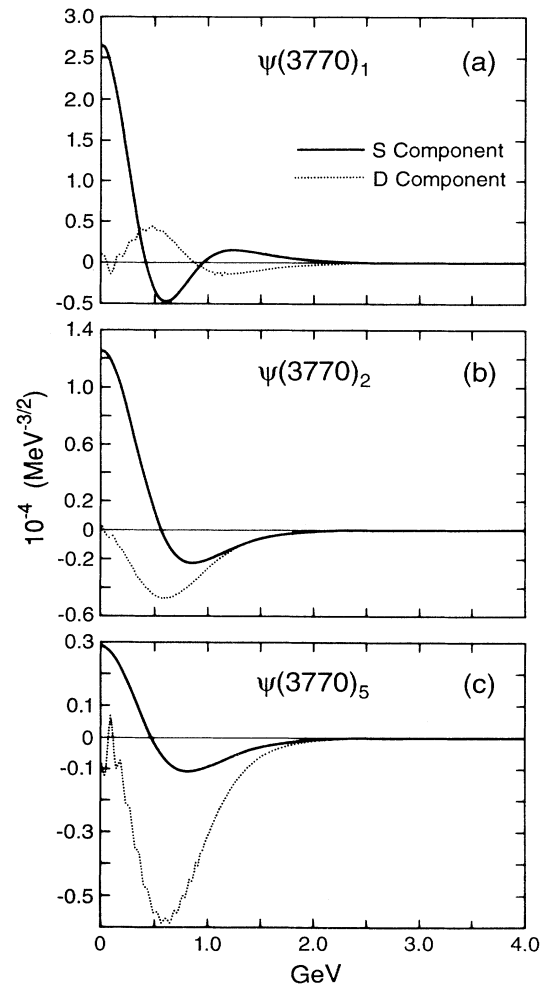


FIG. 6. Wave function of  $\psi(3770)$  for parameter sets (a)1, (b)2, and (c)5.

mental data, including various decay rates, at least electromagnetic and weak. However, the characteristic difference between the Schrödinger formalism and the three-dimensional relativistic equation approach emerges in the numerical study and in the discussion of the asymptotic behavior of the kernel in the region with large but finite momentum. The principal conclusion is that all types of spin-dependent forces which decide the general features of the spectra of the quarkonium system appear to be a higher-order relativistic correction in the Schrödinger approach, but must be considered as an input of the mixing of the various Lorentz covariants in the original BS kernel. The different physical origin of the spin-dependent potential in these two approaches has posed an interesting question in the study of the hadronic structure. The mixing of  $S$  and  $D$  components in the wave function of the  $J/\psi$  system is shown to be sensitive to the presence of the axial-vector and tensor components in the potential.

As far as one would like to continue to study the ha-

dronic wave function of the quark model in momentum space, a serious challenge is to search for a more adequate regularization method for the light-cone singularity in the confinement potential, without which quantitative results are difficult to obtain. The technique developed in this paper can be generalized to the problems of meson states without difficulty. The use of the existing wave functions to calculate various weak decays and transition rates is planned to be presented in papers to follow.

#### ACKNOWLEDGMENTS

We thank A. N. Kamal for many useful discussions. One of the authors (X.Q.Z.) would like to acknowledge H. Y. Chu, A. Czarnecki, Q. Liu, D. Sept, W. W. Wang, B. Xing, and Q. P. Xu for discussions and help with the ongoing work. This work was supported in part by the Natural Sciences and Engineering Research Council of Canada.

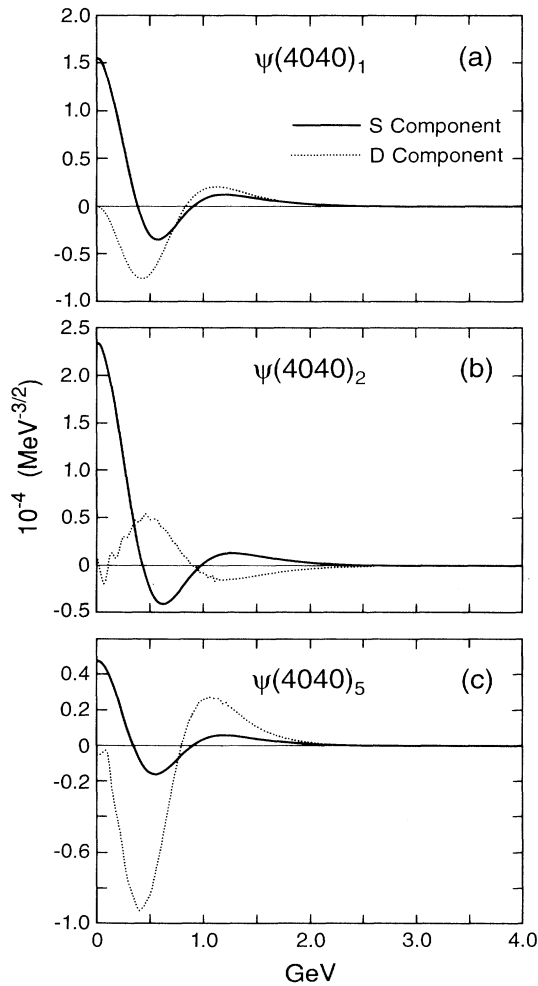


FIG. 7. Wave function of  $\psi(4040)$  for parameter sets (a)1, (b)2, and (c)5.

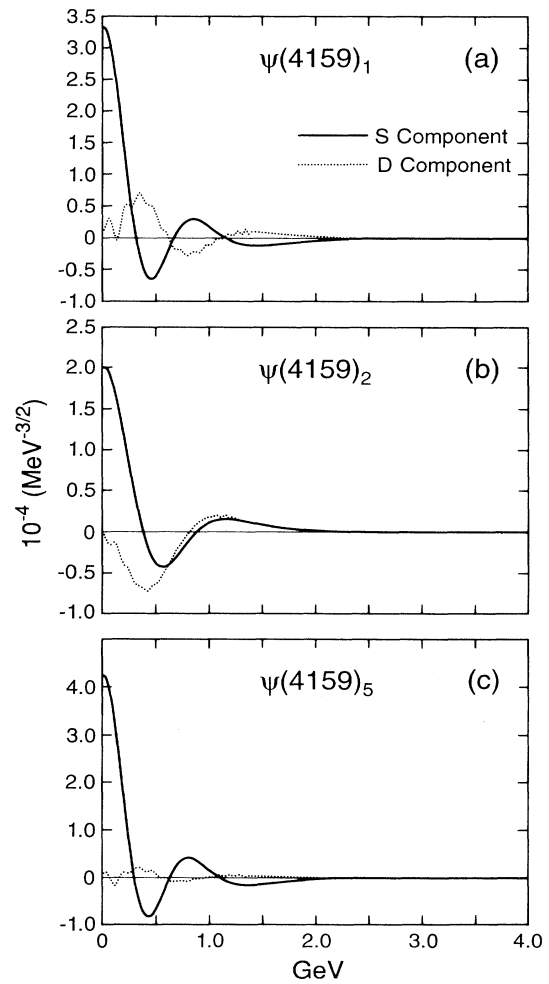


FIG. 8. Wave function of  $\psi(4159)$  for parameter sets (a)1, (b)2, and (c)5.

## APPENDIX A: COVARIANT SPINORS

The unitary representations of the inhomogeneous Lorentz group [15] have been extensively developed for classifying relativistic scattering states. Some of the popular references that deal with the construction of the helicity representation are by Jacob and Wick [16] for general helicity formulation, the  $L$ - $S$  representation by Macfarlane [17], and the relationship of these two representations by McKerrel [18]. Since it is not quite common to use these representations as the basis for a bound-state calculation, it is valuable to collect some of these materials for classifying the basis of the quark-antiquark system. We would like to emphasize that the definition of the phase in the following presentation is crucial in actual calculations. For simplicity of book-keeping, we use  $u^{(\pm)}$  to represent the positive- and negative-energy spinors until we start to discuss two-particle states.

The Dirac spinors in the helicity representation are defined as

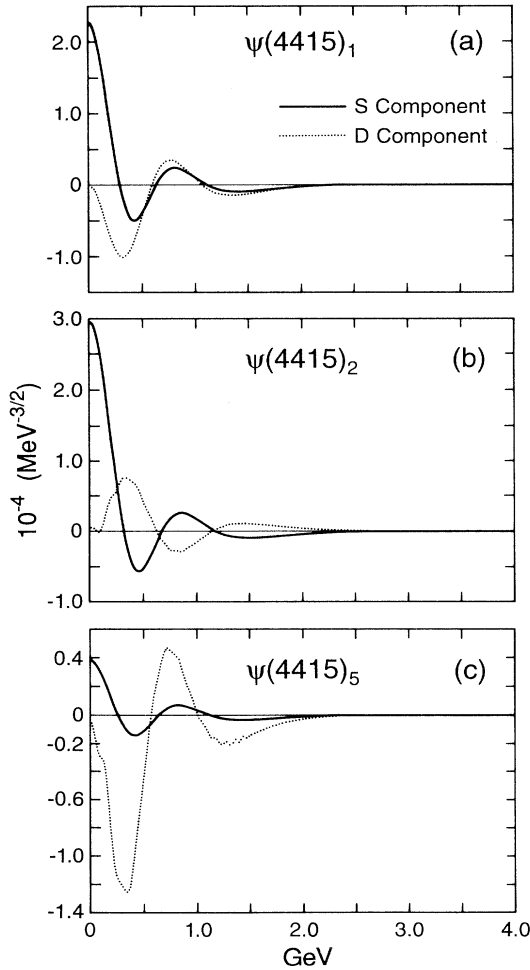


FIG. 9. Wave function of  $\psi(4415)$  for parameter sets (a)1, (b)2, and (c)5.

$$u_H^{(+)}(\mathbf{p}\mu) = \mathcal{L}_H(\mathbf{p})w^+(\mu), \quad (\text{A1})$$

$$u_H^{(-)}(\mathbf{p}\mu) = (-1)^{1/2-\mu} \mathcal{L}_H(\mathbf{p})w^-(-\mu), \quad (\text{A2})$$

$$u_H^{(+)}(-\mathbf{p}\mu) = (-1)^{1/2-\mu} \mathcal{L}_H(-\mathbf{p})w^+(\mu), \quad (\text{A3})$$

$$u_H^{(-)}(-\mathbf{p}\mu) = \mathcal{L}_H(-\mathbf{p})w^-(-\mu), \quad (\text{A4})$$

where  $w^+(\mu) = \begin{pmatrix} x_\mu \\ 0 \end{pmatrix}$  and  $w^-(-\mu) = \begin{pmatrix} 0 \\ x_\mu \end{pmatrix}$ , with  $x_\mu$  being the Pauli spinor.  $\mathcal{L}_H(\pm\mathbf{p})$  is constructed by a boost along the  $z$  direction and, for simplicity, only a rotation around the  $y$  axis:

$$\mathcal{L}_H(\mathbf{p}) = R_y(\theta)L_z(p), \quad (\text{A5})$$

$$\mathcal{L}_H(-\mathbf{p}) = R_y(\theta+\pi)L_z(p), \quad (\text{A6})$$

where

$$L_z(p) = N_p(1 + B_p\alpha^3), \quad (\text{A7})$$

$$R_y(\theta) = \cos\theta/2 - i\sigma^2\sin\theta/2. \quad (\text{A8})$$

Here  $N_p = [(E_p + m)/2E_p]^{1/2}$ ,  $B_p = |\mathbf{p}|/(E_p + m)$ ,  $\alpha^3 = -i\sigma^{03}$ , and  $\sigma^2 = \sigma^{31}$ . The notation and definitions of all Dirac matrices follow Bjorken and Drell [24]. The phase convention in (A2) is introduced subject to the charge-conjugation relation

$$C\bar{u}_H^{(\pm)T}(\mathbf{p}\mu) = u_H^{(\mp)}(\mathbf{p}\mu), \quad (\text{A9})$$

where  $C = i\gamma^2\gamma^0$  and  $T$  indicates transpose operation. The phase in (A3) and (A4) has been chosen such that [16]

$$u_H^{(\pm)}(\mathbf{p}\rightarrow 0, \mu) = u_H^{(\pm)}(-\mathbf{p}\rightarrow 0, -\mu). \quad (\text{A10})$$

The normalization factor in (A7) is chosen to satisfy the condition

$$u_H^{(\pm)\dagger}(\mathbf{p}\mu)u_H^{(\pm)}(\mathbf{p}\mu') = \delta_{\mu\mu'}. \quad (\text{A11})$$

The orthogonality between  $u^{(+)}$  and  $u^{(-)}$  is

$$u_H^{(+)\dagger}(\mathbf{p}\mu)u_H^{(-)}(-\mathbf{p}\mu') = \bar{u}_H^{(+)}(\mathbf{p}\mu)u_H^{(-)}(\mathbf{p}\mu') = 0. \quad (\text{A12})$$

The projection operator for  $u^{(+)}$  and  $u^{(-)}$  can be written as

$$\Lambda^\pm(\mathbf{p}) = \frac{1}{2E_p}[E_p \pm H(\mathbf{p})] = u_H^{(\pm)}(\pm\mathbf{p})u_H^{(\pm)}(\pm\mathbf{p})^\dagger \quad (\text{A13})$$

and satisfies

$$\beta\Lambda^\pm(\mathbf{p}) = \Lambda^\pm(-\mathbf{p})\beta. \quad (\text{A14})$$

The index  $\mu$  of spinors is the eigenvalue of the helicity operator

$$\frac{\boldsymbol{\sigma}\cdot\mathbf{p}}{2}u_H^{(\pm)}(\mathbf{p}\mu) = \pm\mu u_H^{(\pm)}(\mathbf{p}\mu), \quad (\text{A15})$$

where  $\boldsymbol{\sigma}/2$  is the infinitesimal generator of the space rotation (A8). To prove (A15) we have used

$$\boldsymbol{\sigma}\cdot\mathbf{p}R_y(\theta) = R_y(\theta)\sigma_z$$

and note that  $\sigma_z$  commutes with  $L_z(p)$ . Therefore  $\mu$ , the spin projection in the direction of  $\mathbf{p}$ , is the same as the projection on the positive and negative  $z$  axis in the rest

frame for  $u^{(+)}$  and  $u^{(-)}$ , respectively.

The characteristic feature of the helicity representation is that the spinors only rotate the direction of its momentum without changing the spin projection under the rotational transformation

$$R(\omega)u_H^{(\pm)}(\mathbf{p}\mu) = u_H^{(\pm)}(\mathbf{p}'\mu). \quad (\text{A16})$$

Here  $\mathbf{p}' = \Lambda_\omega \mathbf{p}$  and  $\Lambda_\omega$  represent the rotation with a solid angle  $\omega$  in three-dimensional space. The result in Eq. (A16) is evident from the structure of (A5) and (A6).

The space-inversion operation for the spinors is presented as

$$\not{r}u_H^{(r)}(\mathbf{p}\mu) = \eta_r \not{r} \mathcal{L}_H(\mathbf{p}) \not{r}^{-1} \not{r} w^{(r)}(\mu), \quad (\text{A17})$$

where  $r = \pm 1$  and  $\eta_r$  is given by (A1) and (A2). The Lorentz transformation under space inversion is equal to a space rotation around the  $y$  axis by an angle  $\pi$ ,

$$\not{r} \mathcal{L}_H(\mathbf{p}) \not{r}^{-1} = R_y(-\pi) \mathcal{L}_H(\mathbf{p}) R_y(\pi), \quad (\text{A18})$$

and note that

$$\not{r} w^{(r)}(\pm\mu) = \gamma^0 w^{(r)}(\pm\mu) = r w^{(r)}(\pm\mu). \quad (\text{A19})$$

Substituting (A18) and (A19) into (A17) and using

$$R_y(\pi) w^{(r)}(\mu) = (-1)^{1/2 - \mu} w^{(r)}(-\mu),$$

we obtain

$$\not{r} u^{(r)}(\pm\mathbf{p}\mu) = r u^{(r)}(\mp\mathbf{p}, -\mu). \quad (\text{A20})$$

In other words, spinors reverse their momentum and spin projection with an internal parity positive (negative) for  $u^+$  ( $u^-$ ) under space inversion.

In contrast with (A5) and (A6), the definition of the canonical representation of spinors is based on a direct boost from the rest frame to the direction of  $\mathbf{p}$ :

$$u_c^{(+)}(\pm\mathbf{p}\mu) = \mathcal{L}_c(\pm\mathbf{p}) w^{(+)}(\mu), \quad (\text{A21})$$

$$u_c^{(-)}(\pm\mathbf{p}\mu) = (-1)^{1/2 - \mu} \mathcal{L}_c(\pm\mathbf{p}) w^{(-)}(-\mu), \quad (\text{A22})$$

where

$$\mathcal{L}_c(\pm\mathbf{p}) = N_p (1 \pm \mathbf{B}_p \hat{\mathbf{p}} \cdot \boldsymbol{\alpha}). \quad (\text{A23})$$

Consistent with the previous case, we choose  $\hat{\mathbf{p}} = (\sin\theta, 0, \cos\theta)$ . The phase in (A22) is introduced in order to satisfy the charge-conjugation relation (A9).

It can be directly checked that

$$\mathcal{L}_H(\mathbf{p}) = R_y(\theta) \mathcal{L}_z(p) = \mathcal{L}_c(\mathbf{p}) R_y(\theta), \quad (\text{A24})$$

$$\mathcal{L}_H(-\mathbf{p}) = R_y(\pi + \theta) \mathcal{L}_z(p) = \mathcal{L}_c(-\mathbf{p}) R_y(\pi + \theta). \quad (\text{A25})$$

By using these relations and noting that

$$R_y(\theta) w^\pm(\mu) = \sum_\mu d_{\mu\mu'}^{1/2}(\theta) w^\pm(\mu'), \quad (\text{A26})$$

the unitary transformation between the two representations can be obtained:

$$u_H^{(\pm)}(\mathbf{p}\mu) = \sum_{\mu'} d_{\mu\mu'}^{1/2}(\theta) u_c^{(\pm)}(\mathbf{p}\mu'), \quad (\text{A27})$$

$$u_H^{(\pm)}(-\mathbf{p}\mu) = \sum_{\mu'} d_{\mu'\mu}^{1/2}(\theta) u_c^{(\pm)}(-\mathbf{p}\mu'). \quad (\text{A28})$$

The major difference between the two representations is their transformation property under space rotation. Because of the same type of algebra of (A24) and (A25),

$$R(\omega) \mathcal{L}_c(\mathbf{p}) = \mathcal{L}_c(\mathbf{p}') R(\omega), \quad (\text{A29})$$

where  $\mathbf{p}' = \Lambda_\omega \mathbf{p}$ . Applying (A29) and (A26) to (A21) and (A22), we have

$$R(\omega) u_c^{(\pm)}(\mathbf{p}\mu) = \sum_{\mu'} D_{\mu'\mu}^{1/2}(\omega) u_c^{(\pm)}(\mathbf{p}'\mu'). \quad (\text{A30})$$

Comparing (A30) with (A16), the canonical spinors not only transform their direction of  $\mathbf{p}$ , but also the projection of the spin as  $D^{1/2}$  under the Lorentz rotation. Let us define

$$R(\omega) = R^L(\omega) R^S(\omega), \quad (\text{A31})$$

such that

$$R^S(\omega) u_c^{(\pm)}(\mathbf{p}\mu) = \sum_{\mu'} D_{\mu'\mu}^{1/2}(\omega) u_c^{(\pm)}(\mathbf{p}\mu'), \quad (\text{A32})$$

$$R^L(\omega) u_c^{(\pm)}(\mathbf{p}\mu) = u^{(\pm)}(\mathbf{p}'\mu). \quad (\text{A33})$$

The explicit expressions for  $R^S$  and  $R^L$  in terms of Lorentz group elements and the algebra including these two operators can be found in [17]. However, (A31)–(A33) have already been given a unique and precise definition of the orbital and spin rotations. Furthermore, from this definition we can find that  $R^L$  and  $R^S$  commute with each other:

$$[R^S, R^L] = 0. \quad (\text{A34})$$

Now we are ready to turn to the basis states for the quark-antiquark system. From now on we rename  $u^{(-)}$  as  $v$ . First, let us prove Eq. (33). Assuming that the reducible tensor  $X_H(\mathbf{p}\mu_1\mu_2)$  can be decomposed into tensors which are irreducible under the rotation group,

$$X_H(\mathbf{p}\mu_1\mu_2) = \sum_{JM_J} f_{JM_J}(\theta_{\mu_1\mu_2}) X_H(pJM_J\mu_1\mu_2). \quad (\text{A35})$$

Taking  $\mathbf{p}$  in the  $z$  direction at first, i.e.,  $\theta=0$ , we have

$$X_H(p_z\mu_1\mu_2) = \sum_J f_J(\mu_1\mu_2) X_H(pJ\mu_1\mu_2). \quad (\text{A36})$$

Since both spinors on the left-hand side of the equation are in the direction of the  $z$  axis,  $X(p_z\mu_1\mu_2)$  is the eigenstate of  $\sigma_3/2$  with eigenvalue  $\mu = \mu_1 + \mu_2$ . Therefore there is no summation of  $M_J$  on the right-hand side of (A36). Operating from left and right on both sides of Eq. (A36) by the rotation operator  $R_y(\theta)$  and  $R_y^{-1}(\theta)$ , respectively, using the definitions (A1), (A4), and (A5) or using Eq. (A16) and noting that  $R_y(\theta)$  commutes with the  $\gamma^0$  matrix, the left-hand side of (A36) becomes  $X_H(\mathbf{p}\mu_1\mu_2)$ . For the right-hand side of (A36),  $X_H(pJM_J\mu_1\mu_2)$  is supposed to be irreducible under rotations. However, the more important point is that we are working in the c.m. frame of the quark-antiquark system or the rest frame of the system. It is only in the rest frame of the system that

the tensor  $X(pJM_J\mu_1\mu_2)$  transforms like (A26) under rotations

$$R_y(\theta)X_H(pJ\mu_1\mu_2)R_y^{-1}(\theta) = \sum_{M_J} d_{M_J\mu}^J(\theta)X_H(pJM_J\mu_1\mu_2). \quad (\text{A37})$$

Comparing (A37) with (A35), we have

$$f_{JM_J}(\theta\mu_1\mu_2) = f_J(\mu_1\mu_2)d_{M_J\mu}^J(\theta), \quad (\text{A38})$$

where  $f_J(\mu_1\mu_2)$ , independent of  $J$  and  $M_J$ , can be fixed by the normalization condition. Assuming

$$\begin{aligned} \text{Tr}\{X_H^\dagger(p\theta\varphi\mu_1\mu_2)X_H(p\theta'\varphi'\mu'_1\mu'_2)\} \\ = \delta(\cos\theta - \cos\theta')\delta(\phi - \phi')\delta_{\mu_1\mu'_1}\delta_{\mu_2\mu'_2}, \end{aligned} \quad (\text{A39})$$

where we use  $X_H(p\theta\varphi\mu_1\mu_2)$  to indicate the explicit form of  $X_H(\mathbf{p}\mu_1\mu_2)$ . Equation (A39) is a part of the normalization condition for the physical bound states; the normalization concerning the  $|\mathbf{p}|$  will be fixed by the solution of the equation of motion for bound states. Furthermore, as an irreducible representation of the rotation group, we have

$$\begin{aligned} \text{Tr}\{X_H^\dagger(pJM_J\mu_1\mu_2)X_H(pJ'M'_J\mu'_1\mu'_2)\} \\ = \delta_{JJ'}\delta_{M_JM'_J}\delta_{\mu_1\mu'_1}\delta_{\mu_2\mu'_2}. \end{aligned} \quad (\text{A40})$$

Substituting (A35) and (A38) into (A39) and (A40), one can integrate over the angle by using the orthogonality relation of the rotation functions; the final result is

$$f_J(\mu_1\mu_2) = \left[ \frac{2J+1}{4\pi} \right]^{1/2}. \quad (\text{A41})$$

Combining (A35), (A38), and (A41), Eq. (33) has been proved.

Next, in order to prove Eq. (46), we have to go to the canonical representation. Similar to the case of Eq. (31), the  $X$  tensor for a quark-antiquark system in the c.m. frame also can be defined in the canonical representation

$$X_c(\mathbf{p}\nu_1\nu_2) = u_c(\mathbf{p}\nu_1)\bar{v}_c(-\mathbf{p}\nu_2). \quad (\text{A42})$$

Under the spin rotation,  $u_c$  and  $\bar{v}_c$  transform according to the rotation matrix  $D$  and its Hermitian conjugate, respectively [Eq. (A32)], and so we can introduce an irreducible basis with respect to  $R^S$ :

$$X_c(\mathbf{p}SS_z) = \sum_{\nu_1\nu_2} \langle \frac{1}{2}\nu_1\frac{1}{2}-\nu_2 | SS_z \rangle (-1)^{1/2-\nu_2} X_c(\mathbf{p}\nu_1\nu_2). \quad (\text{A43})$$

Equation (A43) also indicates  $S_z = \nu_1 - \nu_2$  in the canonical representation. Using (A32) and (A43), we immediately obtain

$$R^S(\omega)X_c(\mathbf{p}SS_z)R^S(\omega)^\dagger = \sum_{S'_z} D_{S'_z S_z}^S(\omega)X_c(\mathbf{p}SS'_z). \quad (\text{A44})$$

Still,  $X_c(\mathbf{p}SS_z)$  is not irreducible under the transformations  $R^L$ . Under the operation of  $R^L$ , the spinors trans-

form according to (A33), which is exactly like the rotational operator acting in the helicity representation. So we can go through the process as that from (A35) to (A41) for introducing an irreducible representation under  $R^L$  as follows. We define

$$X_c(\mathbf{p}SS_z) = \sum_{L_z} f_{L_z}(\theta)X_c(pLL_zSS_z), \quad (\text{A45})$$

with

$$R^S(\omega)X_c(pLL_zSS_z)R^S(\omega)^\dagger = \sum_{L'_z} D_{L'_z L_z}^L(\omega)X_c(pLL'_zSS_z). \quad (\text{A46})$$

Taking  $\mathbf{p}$  in the direction of the  $z$  axis,

$$X_c(p_zSS_z) = \sum f_L(\theta)X(pL0SS_z). \quad (\text{A47})$$

Again, both spinors on the left-hand side of (A47) are in the  $z$  direction. From (A33) any orbital rotation around the  $z$  axis would not change the spinors which are along the  $z$  direction, i.e.,

$$R^L(\theta)u_c(\mathbf{p}_z\mu) = u_c(\mathbf{p}_z\mu)$$

or

$$\hat{L}_z u_c(\mathbf{p}_z\mu) = 0,$$

where  $\hat{L}_z$  is the infinitesimal operator of  $R_L$  in the  $z$  direction. As a result,  $X_c(p_zSS_z)$  is the eigenstate of  $\hat{L}_z$  with eigenvalue  $L_z = 0$ . Now we can use the operator  $R_y^L(\theta)$  and  $R_y^{L\dagger}(\theta)$  from the left and right on both sides of Eq. (A47) and use the normalization condition to fix the constant with the result

$$X_c(\mathbf{p}SS_z) = \sum_{L_z} \left[ \frac{2L+1}{4\pi} \right]^{1/2} d_{L_z 0}^L(\theta)X(pLL_zSS_z) \quad (\text{A48})$$

and

$$X(pLL_zSS_z) = \left[ \frac{2L+1}{4\pi} \right]^{1/2} \int d\Omega d_{L_z 0}^L(\theta)X_c(\mathbf{p}SS_z). \quad (\text{A49})$$

Noting that  $R^L$  and  $R^S$  commute with each other [Eq. (A34)], the irreducible representation of the total rotation  $R = R^L R^S$  can be defined as

$$X(pJM_JLS) = \sum_{L_z S_z} \langle LL_z SS_z | JM_J \rangle X(pLL_z SS_z). \quad (\text{A50})$$

Using (A44), (A46), and the properties of rotation matrices, we can show that

$$R(\omega)X(pJM_JLS)R^\dagger(\omega) = \sum_{M'_J} D_{M'_J M_J}^J(\omega)X(pJM'_JLS). \quad (\text{A51})$$

Combining (A50), (A49), and (A48), we have

$$X(pJM_JLS) = \left[ \frac{2L+1}{4\pi} \right]^{1/2} \sum_{\nu_1 \nu_2 L_z} \int d\Omega d_{L_z 0}^L(\theta) \langle LL_z SS_z | JM_J \rangle \langle \frac{1}{2} \nu_1 \frac{1}{2} - \nu_2 | SS_z \rangle (-1)^{1/2 - \nu_2} X_c(\mathbf{p}\nu_1\nu_2). \quad (\text{A52})$$

The transformation of  $X_c(\mathbf{p}\mu_1\mu_2)$  into the helicity representation is given already by Eqs. (A27) and (A28) to have the form

$$X_c(\mathbf{p}\nu_1\nu_2) = \sum_{\mu_1\mu_2} d_{\nu_1\mu_1}^{1/2}(\theta) d_{\nu_2-\mu_2}^{1/2}(\theta) X_H(\mathbf{p}\mu_1\mu_2). \quad (\text{A53})$$

Substituting (A53) into (A52) and using expression (34), which relates  $X_H(\mathbf{p}\mu_1\mu_2)$  to  $X_H(pJM_J\mu_1\mu_2)$ , it is a straightforward algebra of  $3j$  symbols and the properties of rotation matrices to get final results given by Eqs. (46) and (47).

## APPENDIX B

The potential in the  $LSJ$  representation ( $LS|V_J(pq)|L'S'$ ) is

$$(00|V_0(pq)|00)/N_p^2 N_q^2 = \{ (1+B_p^2 B_q^2) r_s(1) + (1+B_p^2)(1+B_q^2)[r_v(1)-r_a(1)] - (B_p^2+B_q^2)r_p(1) \\ + (1+B_p^2)(1-B_q^2)r_1(1) \} + 2B_p B_q \{ 2[r_v(2)-r_a(2)] - [r_s(2)-r_p(2)] \}, \quad (\text{B1})$$

$$(11|V_0(pq)|11)/N_p^2 N_q^2 = 2B_p B_q \{ 2[r_v(1)-r_a(1)] - [r_s(1)-r_p(1)] \} \\ + \{ (1+B_p^2 B_q^2) r_s(2) \\ + (1+B_p^2)(1+B_q^2)[r_v(2)-r_a(2)] - (B_p^2+B_q^2)r_p(2) + (1-B_p^2)(1-B_q^2)r_t(2) \}, \quad (\text{B2})$$

$$(10|V_1(pq)|10)/N_p^2 N_q^2 = \{ (1+B_p^2 B_q^2) r_s(2) + (1+B_p^2)(1+B_q^2)[r_v(2)-r_a(2)] - (B_p^2+B_q^2)r_p(2) \\ + (1-B_p^2)(1-B_q^2)r_t(2) \} + 2B_p B_q \{ 2[r_v(3)-r_a(3)] - [r_s(3)-r_p(3)] \}, \quad (\text{B3})$$

$$(11|V_1(pq)|11)/N_p^2 N_q^2 = B_p B_q \{ 4[r_v(1)+r_a(1)] - [r_p(1)+r_s(1)] + 6r_t(1) \} \\ + \{ (1+B_p^2 B_q^2) r_s(2) \\ + (1+B_p^2)(1+B_q^2)[r_a(2)+r_v(2)] + (B_p^2+B_q^2)r_p(2) - (1+B_p^2)(1+B_q^2)r_t(2) \} \\ - B_p B_q \{ r_p(3) + r_s(3) + 2r_t(3) \}, \quad (\text{B4})$$

$$(01|V_1(pq)|01)/N_p^2 N_q^2 = \frac{1}{3} \{ (3-B_p^2 B_q^2) r_s(1) + (3+3B_p^2+3B_q^2-B_p^2 B_q^2) r_v(1) + (1+B_p^2+B_q^2+5B_p^2 B_q^2) r_a(1) \\ + (B_p^2+B_q^2)r_p(1) - (1+3B_p^2+3B_q^2+5B_p^2 B_q^2) r_t(1) \} \\ + \frac{2}{3} B_p B_q \{ 2r_a(2) - r_p(2) - 3r_s(2) + 4r_t(2) + 6r_v(2) \} + \frac{4}{3} B_p^2 B_q^2 \{ r_s(3) - r_a(3) + r_v(3) + r_t(3) \}, \quad (\text{B5})$$

$$(21|V_1(pq)|21)/N_p^2 N_q^2 = \frac{1}{6} \{ (-3+5B_p^2 B_q^2) r_s(1) - (3-3B_p^2-3B_q^2-5B_p^2 B_q^2) r_v(1) + (7+B_p^2+B_q^2-B_p^2 B_q^2) r_a(1) \\ + (B_p^2+B_q^2)r_p(1) - (7+3B_p^2+3B_q^2-B_p^2 B_q^2) r_t(1) \} \\ + \frac{2}{3} B_p B_q \{ -2r_a(2) + r_p(2) - 3r_s(2) + 2r_t(2) + 6r_v(2) \} \\ + \frac{1}{6} \{ (9+B_p^2 B_q^2) r_s(3) + (3+B_p^2)(3+B_q^2)[r_v(3)-r_a(3)] \\ + 3(B_p^2+B_q^2)r_p(3) + (3-B_p^2)(3-B_q^2)r_t(3) \}, \quad (\text{B6})$$

$$(01|V_1(pq)|21)/\sqrt{2} N_p^2 N_q^2 = \frac{1}{3} \{ B_p^2 B_q^2 r_s(1) + (3B_p^2+B_p^2 B_q^2) r_v(1) + (2+2B_p^2-2B_q^2+B_p^2 B_q^2) r_a(1) \\ + (2B_p^2-B_q^2)r_p(1) - (2+3B_p^2+B_p^2 B_q^2) r_t(1) \} + \frac{2}{3} B_p B_q [2r_a(2) - r_p(2) + r_t(2)] \\ + \frac{1}{3} \{ B_p^2 B_q^2 r_s(3) + (3B_p^2+B_p^2 B_q^2)[r_v(3)-r_a(3)] - 3B_q^2 r_a(3) - (3B_q^2-B_p^2 B_q^2) r_t(3) \}, \quad (\text{B7})$$

$$(21|V_1(pq)|01) = (01|V_1(qp)|21), \quad (\text{B8})$$

where the definitions of  $B_p$ ,  $B_q$ ,  $N_p$ , and  $N_q$  are given in Appendix A and

$$r_i(n) = c_i r_c(n) + g_i r_g(n), \quad (\text{B9})$$

where  $c_i$  and  $g_i$  are defined in Eq. (27), where the index  $i$  represents the labels  $s$ ,  $v$ ,  $a$ ,  $p$ , and  $t$ . Here  $r_c(n)$  and  $r_g(n)$  are expressions of the confinement potential and cutoff Coulomb potential integrated over the angle:

$$r_g(n) = \frac{a_c}{2pq} R_c(n), \quad (\text{B10})$$

$$r_c(n) = -\frac{2a_l + 2\mu a_0}{4p^2q^2} R(2, n) + \frac{8a_l\mu^2}{8p^3q^3} R(3, n), \quad (\text{B11})$$

where  $a_c$ ,  $a_l$ , and  $a_0$  are defined by Eqs. (28) and (29) and

$$R_c(n) = \int_{-1}^{+1} dt \frac{t^{n-1}}{z-t} \frac{c^2}{(z-t)^2 + c^2}, \quad (\text{B12})$$

$$R(m, n) = \frac{(-1)^{n-1}}{(n-1)!} \frac{d^{n-1}}{dz^{n-1}} \int_{-1}^{+1} dt \frac{1}{(z-t)^m}. \quad (\text{B13})$$

Here  $z = (1/pq)(E_q E_p - m^2 + \mu^2/2)$ , which is a variable with a value always greater than 1 as long as  $\mu \neq 0$ . Therefore Eqs. (B12) and (B13) are well defined in the infrared region, and the constant  $c = \Lambda_{\text{QCD}}^2/2pq$  takes account of the ultraviolet cutoff in the integration  $R_c(n)$ . The integrals defined in Eqs. (B12) and (B13) have simple expressions in terms of elementary functions.

- 
- [1] S. Godfrey and N. Isgur, *Phys. Rev. D* **23**, 189 (1985).  
 [2] W. Buchmuller, G. Grunberg, and S.-H. H. Tye, *Phys. Rev. Lett.* **45**, 103 (1980); W. Buchmuller and S.-H. H. Tye, *Phys. Rev. D* **24**, 132 (1981).  
 [3] W. Lucha, F. F. Schoberl, and D. Gromes, *Phys. Rep.* **200**, 128 (1991); J. Rosner (unpublished).  
 [4] Y. B. Dai, C. S. Huang, and D. S. Liu, *Phys. Rev. D* **43**, 1717 (1991).  
 [5] R. Alkofer and P. A. Amundsen, *Nucl. Phys.* **B306**, 305 (1988).  
 [6] T. Gudehus, *Phys. Rev.* **184**, 1788 (1969).  
 [7] P. Asthana and A. N. Kamal, *Few Body Syst.* **11**, 1 (1991); F. Hussain, J. G. Körner, and G. Thompson, *Ann. Phys. (N.Y.)* **206**, 334 (1991).  
 [8] R. Blankenbecler and R. Sugar, *Phys. Rev.* **142**, 1051 (1966); V. G. Kadyshesky, *Nucl. Phys.* **B6**, 125 (1968); R. M. Thompson, *Phys. Rev. D* **1**, 110 (1971); K. Erkelenz and K. Holinde, *Nucl. Phys.* **53**, 521 (1969).  
 [9] F. Gross, *Phys. Rev.* **186**, 1448 (1969); *Phys. Rev. C* **26**, 2203 (1982).  
 [10] X. Q. Zhu, R. Gourishankar, F. C. Khanna, G. Y. Leung, and N. Mobed, *Phys. Rev. C* **45**, 959 (1992).  
 [11] A. Klein and T.-S. H. Lee, *Phys. Rev. D* **10**, 4308 (1974);  
 R. Woloshyn and A. D. Jackson, *Nucl. Phys.* **B64**, 269 (1973).  
 [12] C. Llewellyn-Smith, *Ann. Phys. (N.Y.)* **53**, 521 (1964).  
 [13] D. Lurie, A. J. Macfarlane, and Y. Takahashi, *Phys. Rev.* **140**, B1091 (1965).  
 [14] F. Gross and J. Milana, *Phys. Rev. D* **45**, 969 (1992).  
 [15] E. P. Wigner, *Ann. Math.* **40**, 149 (1939).  
 [16] M. Jacob and G. C. Wick, *Ann. Phys. (N.Y.)* **7**, 490 (1959).  
 [17] A. J. Macfarlane, *J. Math. Phys.* **4**, 490 (1963).  
 [18] A. McKerrel, *Nuovo Cimento* **34**, 1289 (1964).  
 [19] Particle Data Group, K. Hikasa *et al.*, *Phys. Rev. D* **45**, S1 (1992).  
 [20] C. Baglin *et al.*, *Phys. Lett. B* **171**, 135 (1986).  
 [21] N. N. Bogoliubov and D. V. Shirkov, *Introduction to the Theory of Quantized Fields*, 3rd ed. (Wiley-Interscience, New York, 1976).  
 [22] N. Isgur and M. B. Wise, *Phys. Lett. B* **232**, 113 (1989); **237**, 527 (1990).  
 [23] K. J. Sebastian, H. Grotch, and F. L. Ridener, Jr., *Phys. Rev. D* **45**, 3163 (1992).  
 [24] J. D. Bjorken and S. D. Drell, *Relativistic Quantum Fields* (McGraw-Hill, New York, 1964).